Journal of Medicinal Chemistry



Article

# Allosteric inhibitors of SHP2 with therapeutic potential for cancer treatment

Jingjing Xie, Xiaojia Si, Shoulai Gu, Mingliang Wang, Jian Shen,
Haoyan Li, Jian Shen, Dan Li, Yanjia Fang, Cong Liu, and Jidong Zhu

*J. Med. Chem.*, **Just Accepted Manuscript** • DOI: 10.1021/acs.jmedchem.7b01520 • Publication Date (Web): 20 Nov 2017



## Just Accepted



ACS Publications

Journal of Medicinal Chemistry is published by the American Chemical Society. 1155 Sixteenth Street N.W., Washington, DC 20036

# Allosteric inhibitors of SHP2 with therapeutic potential for cancer treatment

*Jingjing Xie,* [†,⊥,#] *Xiaojia Si,* [∥,#] *Shoulai Gu,* [†] *Mingliang Wang,* [‡] *Jian Shen,* [†,⊥] *Haoyan Li,* [†,⊥] *Jian Shen,* [§] *Dan Li,* [▽] *Yanjia Fang,* [†] *Cong Liu,* [†,*] *Jidong Zhu* [†,*]

[†]Interdisciplinary Research Center on Biology and Chemistry, Shanghai Institute of Organic Chemistry, Chinese Academy of Sciences, 26 Qiuyue Road, Shanghai 201203, China

[⊥]University of the Chinese Academy of Sciences，19 A Yuquan Road, Shijingshan District，Beijing 100049, China

[‡]Department of Natural Products Chemistry, Fudan University, 826 Zhangheng Road, Shanghai 201203, China

[§]Viva Biotech Ltd. 334 Aidisheng Road, Shanghai 201203, China

[∥]Organisch-Chemisches Institut，Ruprecht-Karls-Universität Heidelberg, Im Neuenheimer Feld 270, 69120, Heidelberg , Germany

[▽]Key laboratory for the Genetics of Developmental and Neuropsychiatric Disorders (Ministry of Education), Bio-X Institutes, Shanghai Jiao Tong University, Shanghai 200240, China

KEYWORDS: SHP2, phosphatase, SH2 domain, allosteric inhibitor, cancer.

## ABSTRACT

SHP2, a cytoplasmic protein-tyrosine phosphatase encoded by the PTPN11 gene, is involved in multiple cell signaling processes including Ras/MAPK and Hippo/YAP pathways. SHP2 has been shown to contribute to the progression of a number of cancer types including leukemia, gastric and breast cancer. It also regulates T-cell activation by interacting with inhibitory immune checkpoint receptors such as the programmed cell death 1 (PD-1) and B- and T-lymphocyte attenuator (BTLA). Thus, SHP2 inhibitors have drawn great attention by both inhibiting tumor cell proliferation and activating T cell immune responses toward cancer cells. In this study, we report the identification of an allosteric SHP2 inhibitor 1-(4-(6-bromonaphthalen-2-yl)thiazol-2-yl)-4-methylpiperidin-4-amine（**23**） that locks SHP2 in a closed conformation by binding to the interface of the N-terminal SH2, C-terminal SH2, and phosphatase domains. **23** suppresses MAPK signaling pathway and YAP transcriptional activity and shows anti-tumor activity *in vivo*. The results indicate that allosteric inhibition of SHP2 could be a feasible approach for cancer therapy.

## INTRODUCTION

Protein tyrosine phosphorylation is a key modification controlling all aspects of crucial cellular processes including proliferation, differentiation, growth and apoptosis. Dysregulation of

tyrosine phosphorylation has been associated with the developmental pathologies of various human diseases such as cancer, diabetes, and autoimmune disorders.[1, 2] Over the past decades, great success has been made to develop protein tyrosine kinase (PTK) inhibitors for clinical application; however, the attempts to develop protein tyrosine phosphatase (PTP) drugs have been hampered due to the less understanding of their biological functions and the poor pharmaceutical properties of PTP inhibitors. Accumulating evidences suggest that some PTPs, such as SHP2, PTP1B, and CDC25, are potential therapeutic targets.[3-5] Thus, developing selective PTP inhibitors may open a new gate accessing more effective therapeutics for human diseases.

SHP2 is a nonreceptor PTP that plays a positive role in cell signaling transduction by growth factors and is involved in cell survival, proliferation and migration.[6-8] Accumulated evidences demonstrate that SHP2 is critical for Ras/MAPK signaling downstream of receptor tyrosine kinases activation.[9-13] SHP2 contains two tandem Src homology 2 (SH2) domains, a PTP domain and a C-terminal tail. At basal state, the N-SH2 domain of SHP2 protein binds to the PTP domain and blocks its substrate access, therefore, resulting in suppressed PTP activity. When the SH2 domains bind to specific phosphotyrosine motifs, the auto-inhibitory interactions are abolished. The phosphatase is then in an open conformation that allows SHP2 activation.[14] Gain-of-function mutations in SHP2 that cause hyperactivation of its catalytic activity have been identified in the developmental disorder Noonan syndrome (～50%)[15, 16] and various cancer types.[17, 18] The mutated residues are located in the interface between N-SH2 and PTP domains. Hyperactivated SHP2 also contributes to tumorigenesis of gastric[19] and breast cancer.[20] SHP2 is implicated in promoting YAP oncoprotein transcriptional activity and stimulating TEAD target

genes.[21] Moreover, SHP2 associates with PD-1 following PD-L1 stimulation and inhibits T cell activation,[22-24] which makes it a promising target for cancer immunotherapy.

Development of small molecule inhibitors targeting PTPs has proven to be considerably difficult due to the highly conserved and positively charged nature of the PTP catalytic domain.[25] Indeed, the previously reported SHP2 inhibitors (**1-7**) have not achieved satisfactory selectivity over other PTPs (Fig.1).[26-32] Until recently, an allosteric inhibitor, **8** (SHP099),[33, 34] was reported to selectively block SHP2 phosphatase activity by stabilizing SHP2 in an auto-inhibited conformation. **8** inhibits cancer cell growth *in vitro* and in mouse tumor xenograft models, demonstrating that inhibition of SHP2 is a valid therapeutic approach for the treatment of cancers. We describe here an independent identification of SHP2 allosteric inhibitors with 2-aminothiazole scaffold through a mutant E76A SHP2 biochemical assay. The inhibitor **23** has an $IC_{50}$ of 700 nM for SHP2 with more than 30-fold selectivity over other PTPs. The co-crystal structure reveals that the inhibitor binds to the same pocket formed by N-SH2, C-SH2 and PTP domains as that identified in **8** case[33, 34]. We show that **23** not only inhibits RAS-ERK signaling, but also suppresses YAP transcriptional activity. **23** inhibits the proliferation of multiple cancer cell lines. In addition, it exhibits acceptable pharmacokinetic properties and inhibits tumor growth in mouse xenograft models, corroborating the potential of SHP2 allosteric inhibitors for the treatment of cancers.

## RESULTS

**Discovery of SHP2 allosteric inhibitors through a mutant E76A SHP2 biochemical screen.** The catalytic sites of protein tyrosine phosphatases are highly conserved and polar, which makes it very challenging to develop selective PTP inhibitors. Recently, a few phosphatase allosteric

inhibitors[35, 36] have been reported to achieve great selectivity and cell permeability, which enlightened us to develop allosteric inhibitors that can freeze SHP2 in its auto-inhibited state. Glutamate 76 plays a key role in bridging N-SH2 and PTP domains, including a hydrogen bond with S502 hydroxyl and a salt bridge interacting with R265. Substituting glutamate 76 leads to weakened interactions between these two domains and thus arouses the destabilization of the auto-inhibited conformation.[37] Mutations of E76 residue have been frequently identified in Noonan syndrome and leukemia.[16] Indeed, mutant E76A full length SHP2 ($SHP2^{E76A}$) exhibited much higher phosphatase activity than wild type SHP2 ($SHP2^{WT}$) in an *in vitro* biochemical assay using DIFMUP as a surrogate substrate. In contrast, C459S SHP2 ($SHP2^{C459S}$)[38], which replaces the catalytic center cysteine to serine, totally abolished its phosphatase activity (Fig. 2A). A biochemical screen against $SHP2^{E76A}$ was conducted with a library of about 20,000 compounds at 20 μM. The hits came from the primary screen were further profiled in a phosphatase assay using SHP2 PTP domain ($SHP2^{PTP}$)[34] to filter out the catalytic inhibitors and non-specific binders. One compound, **9** (Fig. 2B), was identified to show inhibition against $SHP2^{E76A}$ with an $IC_{50}$ of 19.1 μM, but no effect on $SHP2^{PTP}$ (Fig. 2C). Thus, **9** could serve as a starting point to develop SHP2 allosteric inhibitors. We speculated that the amine part may gain certain hydrogen bonds critical for the interaction. Therefore, we kept the amine part intact and enriched the complexity of **9** by changing the phenyl with several common aryl groups. A brief replacement of phenyl with biphenyl (**10** and **11**) or naphthyl (**12**) led to improved potency with $IC_{50}$ of 3.27, 5.32 and 2.55 μM, respectively (Fig. 2D).

**The atomic structure of SHP2 in complex with 10.** To elucidate the structural basis underlying recognition of inhibitors to SHP2, we determined the crystal structure of $SHP2^{E76A}$ in complex with **10** (Table 1). $SHP2^{E76A}$ adopted an auto-inhibited conformation as previously observed in

wild-type SHP2 and SHP2$^{E76Q}$ structures (Fig. 3A)[14, 37, 39]. **10** is accommodated in the same pocket, as previously described for **8** but with distinct binding features (Fig. 3B)[31,32]. The amino linker of **10** forms hydrogen bond with main-chain carbonyl of Arg111 and the methyl groups of tetramethylpiperidine make several van der Waals contacts with Thr108, Glu110, His114, Glu249, and Thr253. The diphenyl moiety is sandwiched between side-chains of Arg111 and Lys492 via cation-π interaction[34], and the hydrophobic patch formed by the side chains of Leu254, Gln257, Pro491 and Gln495 further stabilizes the diphenyl moiety (Fig. 3C). Compared with the 6-member aminopyrazine core in **8**, the 5-member thiazole core of **10** provides a different trajectory for both the aryl and the piperidine regions, which may result in distinct structure-activity relationship (SAR). The hydrogen bond between the amino linker and Arg111 is unique to **10**, although this interaction is relatively weak as indicated by the 3.5Å distance between the donor and the acceptor, possibly due to the steric hindrance between the tetramethylpiperidine group and side-chain of His114. The cation-π interaction by diphenyl moiety is more toward the terminal phenyl ring and involves both Arg111 and Lys492, consistent with the 6-fold increase of potency from **9** to **10**. The central binding pocket located in the interface of the three domains (Fig.S1) is within the hinge region of SHP2 ， which is proposed to rearrange upon substrate binding. From SHP1 structures,[40] the hinge region is observed to undergo dramatic conformational changes to release PTP from N-SH2 domain for substrate binding (Fig. S1). The binding of **10** in the central pocket of SHP2 locks the hinge region and prevents the substrate binding and phosphatase activity of PTP domain by allosteric regulation. Thus, the complex structure provided structural basis of allosteric inhibition of **10** to SHP2 which served as a guideline for improvement of allosteric inhibitors with higher potency by structure-based design.

**SAR analysis of SHP2 inhibitors.** Intrigued by the complex structure of **10** with $SHP2^{E76A}$, we turned our focus to improve its potency. Since the aminothiazole core of **10** provides a different binding trajectory compared with **8**, we decided to maintain the aminothiazole core and independently explore the SAR of the aryl and the piperidine regions (Scheme 1 and Scheme 2).

In our approach to build SAR on amine regions, we synthesized 2-bromo-4-(naphthalene-2-yl)thiazole (**38d**, Scheme 1) as a key intermediate to enrich the diversity of amine by Buchwald reaction. The commercial available amines were coupled with **38d** followed by deprotection when necessary as exampled in Scheme 1. Similarly, in order to explore SAR on the aryl substitutions, a different synthetic approach (Scheme 2) was deployed. Dibromothiazole **43** was substituted with amine (exampled as **44**, Scheme 2) followed by Suzuki coupling with various boronic acids, to afford compounds **20-22, 25, 28-35**.

The brief SAR was summarized in Table 2 and Table 3. Removal of four methyl groups in piperidine increased compound activity by 3.5 fold (Table 2, e.g., **12**, **13**), likely due to the improved H-bond interaction between the amino linker and Arg111 by removing the steric hindrance to His114. Increasing the nitrogen substitution reduced inhibition (e.g., **13**, **14**), suggesting the terminal NH group may be involved in important interactions such as hydrogen bond with surrounding residues, which most likely involve water molecules since we did not observe any direct interaction in the crystal structure. Replacement of piperidine with pyrrolidine or adding one $CH_2$ in N linker is tolerable for SHP2 inhibition (e.g., **15**, **16**). We then directly linked thiazole with piperidine. Compound **17** compensates the loss of hydrogen-bond between the amino linker and Arg111 with a potentially more favorable hydrogen-bonding interaction by the terminal NH2 group, resulting in slightly improved activity as compared to **12**. The amine functional group of **17** is same as that of **8**, suggesting the amino group is optimal to capture the

H-bond interactions with surrounding residues.[34] Other substitutions on piperidine resulted in compromised activity against SHP2 (e.g., **18**, **19**). Compound **12-17** showed comparable activity, however, some of the compounds (e.g. **13**) were not stable in DMSO solution even at -20$^{o}$C stock. **17** showed stable chemical stability and good bioactivity, therefore, we chose compound **17** as a template to further optimize the aryl region. In general, substitutions on naphthaline such as F, Cl, Br, OMe, CN and $CO_2Me$ were well accepted to inhibit SHP2, suggesting the hydrophobic cleft is tolerable to electron donating and withdrawing groups (Table 3, e.g., **20-25**). However, polar substitutions with acid or hydroxyl abolished the compound activity, consistent to the non-polar environment of the hydrophobic cleft (e.g., **26**, **27**). The potency of 1, 3-diphenyl substitutions was generally better than that of 1, 4-diphenyl, suggesting that the terminal phenyl in 1, 3-diphenyl adopted a favorable position for pi-cation interaction with the side chain of Arg111 (e.g., **28-32**). Other aryl groups we tested led to dramatic reduced inhibition against SHP2 (**33-35**). After two rounds of optimization and SAR study, we identified compound **23** as a SHP2 allosteric inhibitor with an $IC_{50}$ of 0.7 μM for $SHP2^{E76A}$, but no inhibition on $SHP2^{PTP}$ (Fig. S2).

To compare the reported biochemical assay using $SHP2^{WT}$ stimulated with 2P-IRS-1 peptide [31, 32] with that using $SHP2^{E76A}$ in this study, we tested **23** and **8** in both assay formats (Fig. S3). **8** exhibited an $IC_{50}$ of 0.06 μM for $SHP2^{WT}$ (2P-IRS-1) and 0.12 μM for $SHP2^{E76A}$. Similarly, **23** showed comparable $IC_{50}$s in the two assays, suggesting that both assays are able to identify SHP2 allosteric inhibitors with similar sensitivity. Selectivity profiling revealed that **23** exhibited more than 30-fold selectivity over other PTPs, including LmwPTP, MKP3, PTP1B, TC-PTP, et al. (Table 4). Of particular note, **23** displayed a 48-fold preference for SHP2 over its closely related homologue SHP1.

**23 inhibits MAPK signaling pathway and antagonizes YAP transcription activity.** To examine if **23** could interfere with ERK activation in cancer cells, we treated a large-cell lung carcinoma cell line NCI-H661 with **23** at indicated concentrations. NCI-H661 cells harbor SHP2 N58S gain-of-function mutation, whose activity was inhibited by **23** with an $IC_{50}$ of 1.2 μM (Fig. S4). As shown in Fig 4A, the levels of both phosphorylated ERK and AKT were downregulated upon **23** treatment, whereas the inactive compound **34**, had no effect even at 20 μM (Fig. 4A). The inhibition of ERK activation by **23** was time-dependent, reaching max inhibition at 60min (Fig. 4B). SHP2 plays a key role in RAS-MAPK activation mediated by receptor tyrosine kinases[9-13]. We then tested **23** in H1975 cells harboring the T790M mutation in EGFR, whose proliferation was reported to be dependent on SHP2.[41] Treatment of **23** diminished the immunofluorescence of p-ERK1/2, indicating that **23** effectively blocked MAPK signaling pathway mediated by activated SHP2 (Fig. 4C).

SHP2 has been shown to physically associate with the oncoprotein YAP and potentiate its transcriptional coactivator function.[21] Indeed, we found that Flag-YAP could be co-immunoprecipitated by HA-SHP2 and *vice versa* in HEK293T cells (Fig. 5A). To ask if SHP2 phosphatase activity is involved in regulation of Hippo/YAP signaling pathway, we then tested **23** in a YAP-dependent luciferase reporter assay. SF268, a neuroblastoma cell line harboring YAP amplification, was stably expressed with a luciferase reporter driven by YAP responsive promoter. The luciferase activity was decreased by **23** treatment in a dose-dependent manner, but not by the negative compound **34** (Fig. 5B). Moreover, the mRNA levels of YAP target genes *CTGF*, *CYR61* and *ANKRD1*[42], but not YAP itself, were downregulated by the treatment of **23** (Fig. 5C). Notably, **23** elevated the level of tyrosine phosphorylation on YAP (Fig. 5D). It has been shown that c-Abl antagonizes the YAP oncogenic function by phosphorylating YAP at

Y357.[43] We then asked if SHP2 could regulate YAP Y357 phosphorylation. Indeed, treatment of A549 cells harboring KRAS mutation with **23** increased Y357 phosphorylation (Fig. 5E), while p-ERK1/2 was not obviously affected. To further investigate whether YAP is a direct substrate of SHP2, we performed *in vitro* dephosphorylation assay using phosphorylated Y357 peptide. $SHP2^{E76A}$ decreased the phosphorylation level of the peptide, which was reversed in the presence of **23** (Fig. 5F).

**23 inhibits cancer cell proliferation *in vitro* and tumor growth *in vivo*.** Because **23** effectively inhibited pro-survival and pro-growth signaling pathways such as MAPK and YAP, we then examined its effect on cancer cell proliferation. We tested **23** activity in a panel of cancer cell lines including lung, breast, esophageal and hematopoietic tumors. The SHP2 inhibitor exhibited a broad anti-tumor activity with great potency in a subset of leukemia cell lines such as MV4;11 and MOLM-13 which contain FLT3-ITD mutation (Fig. 6A). **23** also attenuated the colony formation of H1975 cells, showing that **23** inhibited anchorage-independent cancer cell growth (Fig. 6B).

Pharmacokinetics studies revealed that **23** had good oral exposure (10 mg/kg PO AUC: 9860 nM •h) and bioavailability (67% F) with half-life of 13.3 h (Table S1). The promising PK properties stimulated us to further evaluate the anti-tumor activity of **23** *in vivo*. We chose MV4;11 cells to establish a xenograft model by subcutaneously implanting cells into immunocompromised mice. A daily oral dose of 10 or 30 mg/kg of **23** led to 44.6% and 56.0% tumor growth inhibition, respectively, while the body weight was not significantly affected (Fig. 6C). The tumor volumes on the last day of treatment and the statistical analysis were presented in Fig 6D.

## DISCUSSION AND CONCLUSION

SHP2 has drawn great attention as an anti-tumor target due to its direct genetic link to cancer and critical function in pro-survival signaling pathways. In our study, we established a new screen strategy for SHP2 allosteric inhibitors using $SHP2^{E76A}$ protein and successfully discovered **9** as a novel allosteric inhibitor of SHP2. Further optimization led to a more potent compound **23** with an $IC_{50}$ of 0.7 μM. The $IC_{50}$s of **23** or **8** in $SHP2^{E76A}$ and $SHP2^{WT}$ (2P-IRS-1) biochemical assays were comparable (Fig. S3), suggesting that either assay format can serve as a feasible approach to identify SHP2 allosteric inhibitors. **23** effectively suppressed ERK1/2 and AKT activation in cancer cells. SHP2 has been involved in regulation of YAP oncogene transcriptional activity; however, it is not elucidated if the regulation is SHP2 phosphatase activity dependent. Our data showed that **23** inhibited YAP-dependent reporter and the expression of YAP target genes, suggesting that YAP activity is modulated by SHP2 PTP catalytic function. **23** inhibited the proliferation of a variety of cancer cell lines and suppressed the colony formation of lung cancer cell H1975. It exhibited good PK profiling and anti-tumor activity in a MV4;11 xenograft model. Our study described herein corroborates that allosteric inhibition of SHP2 could be a feasible approach to develop novel anticancer therapies.

## EXPERIMENTAL SECTION

**Materials.** DIFMUP (6,8-Difluoro-4-Methylumbelliferyl Phosphate) was purchased from Thermo Fisher Scientific. Rabbit antiphospho-AKT, antitotal AKT, antiphospho-ERK1/2, antitotal ERK1/2 and mouse antiphosphotyrosine pY-100 were purchased from Cell Signaling Technology. Mouse anti-YAP was from Santa Cruze Biotechnology. And rabbit antiphospho-YAP(Y357) was from Abcam.

**General Methods for Chemistry.** All reagents and starting materials were obtained from commercial suppliers and used without further purification unless otherwise stated. Reaction progress was monitored by thin layer chromatography (TLC) on preloaded silica gel 60 F254 plates. Visualization was achieved with UV light and iodine vapor. All reactions involving oxygen- or moisture-sensitive compounds were carried out under a dry $N_2$ atmosphere. THF was distilled from sodium/benzophenone immediately prior to use. Toluene was distilled from sodium immediately prior to use. Yields were of purified product and were not optimized. $^1$H NMR, $^{13}$C NMR were recorded on Bruker AM-400, Agilent-NMR-vnmrs 400 spectrometers in the corresponding solvent. $^1$H NMR spectra were referenced to the residual solvent peaks as internal standards (7.26 ppm for $CDCl_3$, 2.50 ppm for DMSO-$d_6$, and 3.34 ppm for $CD_3OD$). $^{13}$C NMR spectra were referenced to the residual solvent peaks as internal standards (39.52 ppm for DMSO-$d_6$), NMR data were recorded as follows: multiplicity (s = singlet, d = doublet, t =triplet, m = multiplet or unresolved, coupling constant (solid) in Hz, integration). Mass spectra were determined on an Agilent 5973N MSD (EI), Shimadzu LCMS-2010EV (ESI) mass spectrometer or Agilent G6100 LC/MSD (ESI) single Quand mass spectrometer and IonSpec HiResMALDI. High resolution mass spectra were recorded on Waters Micromass GCT Premier (EI), Bruker Daltonics, Inc. APEXIII 7.0 TESLA FTMS (ESI) mass spectrometers and IonSpec 4.7 Tesla FTMS (MALDI). The purity was determined by high performance liquid chromatography (HPLC). Purity of all final compounds was 95% or higher. The instrument was an Agilent Technologies 6120 LC/MS system. The column was a Phenomenex Luna C18, 100A, 2.0 50mm, 5um.

***General Procedure A: Buchwald−Hartwig Coupling.*** To an oven-dried round-bottomed flask equipped with a stir bar was added $Pd_2(dba)_3$ (23 mg, 0.025 mmol,5 mol %), Xantphos (29 mg,

0.05 mmol,10 mol %), sodium tert-butoxide (96 mg, 1.0 mmol, 2.0 equiv), and the aryl bromide (0.5 mmol, 1.0 equiv). Toluene (0.5M) was added followed by the amine (1.5 mmol, 3.0 equiv), and the reaction mixture was degassed by sparging with $N_2$(g) for 10 min, and the resulting suspension was heated at 120 °C for 3-12 h, the reaction mixture was allowed to cool to r.t, then diluted with ethyl acetate and subsequently filtered with celite. After the filtrate was concentrated under reduced pressure, the resulting residue was purified by chromatography as specified.

***General Procedure B: Suzuki-Coupling and Boc-deprotection.*** The corresponding brominated aromatic compound (0.5 mmol, 1.0 equiv) was dissolved in THF (10 mL/ mmol), the corresponding boronic acid or boronic acid ester (0.6 mmol,1.2 equiv) and an aqueous 2.0 M $Na_2CO_3$ solution (0.75 mL, 3.0 equiv) were added. The mixture was deoxygenated under reduced pressure and flushed with nitrogen. After having repeated this cycle several times, $Pd(PPh_3)_4$ (29 mg, 0.025 mmol, 5 mol %) was added, and the resulting suspension was heated at 80 °C for 12−16 h. After cooling, ethyl acetate and water were added and the organic phase was separated. The water phase was extracted with ethyl acetate. The combined organic phases were washed with brine, dried over $Na_2SO_4$, concentrated in vacuo, and purified by chromatography to afford Boc-protected product, which was treated with trifluoroacetic acid to get Boc-deprotected product.

***4-Phenyl-N-(2, 2, 6, 6-tetramethylpiperidin-4-yl)thiazol-2-amine (9)***. The title compound was prepared from **38a** and 2,2,6,6-tetramethylpiperidin-4-amine following general procedure A. Yellow solid (66 mg,42% yield ). $^1$H NMR (400 MHz, DMSO-$d_6$) δ ppm 9.37 (s, 1H), 7.85 – 7.80 (m, 3H), 7.37 (t, *J* = 7.6 Hz, 1H), 7.26 (t, *J* = 7.2 Hz, 1H), 7.10 (s, 1H), 4.18-4.11 (m, 1H), 2.13 (dd, *J* = 3.2 Hz, *J* = 5.2 Hz,2H), 1.59-1.53 (m, 2H), 1.47 (d, *J* = 18.4 Hz, 12H); $^{13}$C NMR (100 MHz, DMSO-$d_6$) δ ppm 166.88, 149.77, 134.80, 128.47, 127.30, 125.59, 101.26, 56.68,

45.11, 40.54, 29.73, 24.26; HRMS-ESI: calcd. for $C_{18}H_{26}N_3S$ [M + H]$^+$: 316.1842, found: 316.1845.

***4-([1,1'-Biphenyl]-3-yl)-N-(2,2,6,6-tetramethylpiperidin-4-yl)thiazol-2-amine (10)***. The title compound was prepared from **38b** and 2,2,6,6-tetramethylpiperidin-4-amine following general procedure A. Yellow solid (90 mg, 46% yield). $^1$H NMR (400 MHz, DMSO-d$_6$) δ ppm 8.15 (s, 1H), 7.82 (d, *J* = 8.0 Hz, 1H), 7.69 (d, *J* = 7.2 Hz, 1H), 7.61-7.55 (m, 2H), 7.49-7.44 (m, 3H), 7.40-7.34 (m, 1H), 7.19 (s, 1H), 4.03-3.90 (m, 1H), 1.97 (dd, *J* = 2.4 Hz, *J* = 12.0 Hz, 2H), 1.25 (s, 6H), 1.09 (s, 6H), 1.05-0.98 (m, 2H); $^{13}$C NMR (100 MHz, DMSO-d$_6$) δ ppm 167.36, 149.66, 140.29, 140.18, 135.52, 129.12, 128.91, 127.52, 126.63, 125.51, 124.54, 124.03, 101.04, 51.04, 47.71, 43.91, 34.04, 28.19; HRMS-ESI: calcd. for $C_{24}H_{30}N_3S$ [M + H]$^+$: 392.2155, found: 392.2153.

***4-([1,1'-Biphenyl]-4-yl)-N-(2,2,6,6-tetramethylpiperidin-4-yl)thiazol-2-amine (11).*** The title compound was prepared from **38c** and 2,2,6,6-tetramethylpiperidin-4-amine following general procedure A. Yellow solid (100 mg, 51% yield). $^1$H NMR (400 MHz, DMSO-d$_6$) δ ppm 9.38 (s, 1H), 7.93 (d, *J* = 8.4 Hz, 2H), 7.83 (d, *J* = 7.2 Hz, 1H), 7.71-7.68 (m, 4H), 7.47 (t, *J* = 7.6 Hz, 1H), 7.36 (t, *J* = 7.6 Hz, 1H), 7.17 (s, 1H), 4.22-4.12 (m, 1H), 2.14 (dd, *J* = 2.4 Hz, *J* = 13.2 Hz, 2H), 1.56-1.40 (m, 14H); $^{13}$C NMR (100 MHz, DMSO-d$_6$) δ ppm166.93, 149.42, 139.70, 138.81, 133.93, 128.95, 127.74, 126.70, 126.16, 101.54, 56.63, 45.17, 40.60, 29.81, 24.33; HRMS-ESI: calcd. for $C_{24}H_{30}N_3S$ [M + H]$^+$: 392.2155, found: 392.2157.

***4-(Naphthalen-2-yl)-N-(2, 2, 6, 6-tetramethylpiperidin-4-yl) thiazol-2-amine (12)***. The title compound was prepared from **38d** and 2,2,6,6-tetramethylpiperidin-4-amine following general procedure A. White solid (97 mg, 53% yield). $^1$H NMR (400 MHz, DMSO-*d*$_6$) δ ppm 8.35 (s,

1H), 7.98 (dd, *J* = 4.0 Hz, *J* = 8.0 Hz, 1H ), 7.90-7.83 (m, 3H), 7.65 (d, *J* = 8.0 Hz,1H), 3.98-3.94 (m, 1H), 1.95 (dd, *J* = 4.0 Hz, *J* = 8.0 Hz, 1H ), 1.24 (s, 6H), 1.09-1.03 (m, 8H); $^{13}$C NMR (100 MHz, DMSO-$d_6$) δ ppm 167.62, 149.87, 133.16, 132.43, 132.35, 128.07, 127.93, 127.58, 126.38, 125.83, 124.08, 101.40, 50.81, 48.08, 44.24, 34.42, 28.52 . HRMS-ESI: calcd. for $C_{22}H_{28}N_3S$ [M + H]$^+$: 366.1998, found: 366.1995.

***4-(Naphthalen-2-yl)-N-(piperidin-4-yl)thiazol-2-amine (13).*** The title compound was prepared from **38d** and piperidin-4-amine following general procedure A. Yellow solid (56 mg, 36 % yield). $^1$H NMR (400 MHz, $CDCl_3$) δ ppm 8.32 (s, 1H), 7.98 – 7.72 (m, 4H), 7.46-7.44 (m, 2H), 6.81 (s, 1H), 5.52 (s, 1H), 3.53 (s, 1H), 3.13 (d, *J* = 12.0 Hz, 2H), 2.74 (t, *J* = 11.3 Hz, 2H), 2.48 (s, 1H), 2.15 (d, *J* = 11.3 Hz, 2H), 1.52-1.41 (m, 2H); $^{13}$C NMR (101 MHz, DMSO-$d_6$) δ ppm 167.06, 149.85, 133.15, 132.36, 132.29, 128.02, 127.89, 126.35, 125.83, 124.14, 124.06, 102.12, 48.73, 41.78, 21.13; HRMS-ESI: calcd. for $C_{18}H_{20}N_3S$ [M + H]$^+$: 310.1372, found: 310.1369.

***N-(1-methylpiperidin-4-yl)-4-(naphthalen-2-yl)thiazol-2-amine (14)***. The title compound was prepared from **38d** and 1-methylpiperidin-4-amine following general procedure A. Yellow solid (79 mg, 49 % yield). $^1$H NMR (400 MHz, $CDCl_3$) δ ppm 8.29 (s, 1H), 7.88 – 7.79 (m, 4H), 7.49 – 7.40 (m, 2H), 6.80 (s, 1H), 5.88 (s, 1H), 3.71 (s, 1H), 3.13 – 3.09 (m, 2H), 2.58 – 2.43 (m, 5H), 2.26 (d, *J* = 11.7 Hz, 2H), 1.96-1.85 (m, 2H); $^{13}$C NMR (101 MHz, DMSO-$d_6$) δ ppm 167.31, 149.88, 133.15, 132.35, 132.34, 128.03, 127.89, 126.34, 125.81, 124.15, 124.01, 101.87, 54.92, 52.94, 44.40, 30.06; HRMS-ESI: calcd. for $C_{19}H_{22}N_3S$ [M + H]$^+$: 324.1529, found: 324.1531.

***4-(Naphthalen-2-yl)-N-(pyrrolidin-3-yl)thiazol-2-amine (15).*** The title compound was prepared from **38d** and pyrrolidin-3-amine following general procedure A. Yellow solid (60 mg, 41 % yield). $^1$H NMR (400 MHz, DMSO-$d_6$) δ ppm 9.40 (s, 1H), 8.37 (s, 1H), 8.13 (d, *J* = 5.2 Hz,

1H), 7.99 (d, *J* = 1.2 Hz, *J* = 8.4 Hz, 1H), 7.94-7.88 (m, 3H), 7.53-7.46 (m, 2H), 7.30 (s, 1H), 4.49-4.43 (m, 1H), 3.57-3.52 (m, 1H), 3.39-3.26 (m, 3H), 2.33-2.24 (m, 1H), 2.07-2.00 (m, 1H); $^{13}$C NMR (100 MHz, DMSO-$d_6$) δ ppm 167.59, 150.33, 133.63, 132.87, 132.61, 128.52, 128.45, 128.05, 126.87, 126.37, 124.59, 124.57, 103.38, 53.83, 49.85, 43.98, 30.55; HRMS-ESI: calcd. for $C_{17}H_{18}N_3S$ $[M + H]^+$: 296.1216, found: 296.1213.

***4-(Naphthalen-2-yl)-N-(piperidin-3-ylmethyl)thiazol-2-amine (16).*** Following the general procedure A from **38d** and *tert*-butyl 3-(aminomethyl)piperidine-1-carboxylate to afford *tert*-butyl 3-(((4-(naphthalen-2-yl)thiazol-2-yl)amino)methyl)piperidine-1-carboxylate, which was treated with trifluoroacetic acid to get compound **16**. Yellow solid (58 mg, 36 %yield). $^1$H NMR (400 MHz, DMSO-$d_6$) δ ppm 8.92 (s, 1H), 8.36 (s, 1H), 7.99-7.87 (m, 4H), 7.53-7.45 (m, 2H), 7.22 (s, 1H), 3.22-3.19 (m, 2H), 2.80-2.65 (m, 2H), 2.18-2.14 (m, 1H), 1.87-1.80 (m, 2H), 1.67-1.64 (m, 2H), 1.30-1.23 (m, 2H); $^{13}$C NMR (100 MHz, DMSO-$d_6$) δ ppm 168.44, 149.85, 133.18, 132.37, 132.32, 128.09, 127.91, 127.57, 126.36, 125.85, 124.15, 124.12, 101.96, 47.33, 46.42, 43.36, 33.56, 26.11, 21.50; HRMS-ESI: calcd. for $C_{19}H_{22}N_3S$ $[M + H]^+$: 324.1529, found: 324.1527.

***4-Methyl-1-(4-(naphthalen-2-yl)thiazol-2-yl)piperidin-4-amine (17).*** Following the general procedure A from **38d** and *tert*-butyl (4-methylpiperidin-4-yl)carbamate to afford tert-butyl (4-methyl-1-(4-(naphthalen-2-yl)thiazol-2-yl)piperidin-4-yl)carbamate, which was treated with trifluoroacetic acid to get compound **17**. White solid (73 mg, 45% yield). $^1$H NMR (400 MHz, DMSO-$d_6$) δ ppm 8.44 (s, 1H), 8.40 (s, 1H), 8.32 (s, 2H), 8.01-7.89 (m, 4H), 7.53-7.47 (m, 2H), 7.44 (s, 1H), 3.88-3.84 (m, 2H), 3.46-3.36 (m, 2H), 1.94-1.90 (m, 2H), 1.83-1.80 (m, 2H), 1.40 (s, 3H) ; $^{13}$C NMR (100 MHz, DMSO-$d_6$) δ ppm 170.05, 150.56, 133.16, 132.48, 132.08, 128.10,

128.02, 127.59, 126.45, 125.98, 124.24, 124.08, 103.60, 51.80, 44.13, 33.76, 22.06; HRMS-ESI: calcd. for $C_{19}H_{22}N_3S$ $[M + H]^+$: 324.1529, found: 324.1525.

***2-(3,5-Dimethylpiperazin-1-yl)-4-(naphthalen-2-yl)thiazole (18).*** Following the general procedure A from **38d** and *tert*-butyl 2,6-dimethylpiperazine-1-carboxylate to afford *tert*-butyl 2,6-dimethyl-4-(4-(naphthalen-2-yl)thiazol-2-yl)piperazine-1-carboxylate, which was treated with trifluoroacetic acid to get compound **18**. White solid (76 mg, 47% yield). $^1$H NMR (400 MHz, DMSO-$d_6$) δ ppm 8.40 (s, 1H), 8.01-7.89 (m, 4H), 7.53-7.46 (m, 2H), 7.44 (s, 1H), 3.95 (dd, $J$ = 2.4 Hz, $J$ = 12.0 Hz,2H), 3.07 (s, 2H), 2.77 (t, $J$ = 11.2 Hz, 2H), 1.17 (d, $J$ = 6.0 Hz, 6H); $^{13}$C NMR (100 MHz, DMSO-$d_6$) δ ppm 170.08, 150.50, 133.14, 132.46, 132.05, 128.09, 127.98, 127.56, 126.40, 125.95, 124.23, 124.08, 103.48, 53.00, 50.02, 17.70; HRMS-ESI: calcd. for $C_{19}H_{22}N_3S$ $[M + H]^+$: 324.1529, found: 324.1525.

***(1-(4-(Naphthalen-2-yl)thiazol-2-yl)piperidin-3-yl)methanamine (19).*** Following the general procedure A from **38d** and *tert*-butyl(piperidin-3-ylmethyl)carbamate to afford *tert*-butyl 2,6-dimethyl-4-(4-(naphthalen-2-yl)thiazol-2-yl)piperazine-1-carboxylate, which was treated with trifluoroacetic acid to get compound **19**. White solid (69mg, 43% yield). $^1$H NMR (400 MHz, DMSO-$d_6$) δ ppm 8.42 (s, 1H), 8.01 (dd, $J$ = 2.0 Hz, $J$ = 8.8 Hz, 1H), 7.95-7.89 (m, 3H), 7.54-7.47 (m, 2H), 7.44 (s, 1H), 4.10 (dd, $J$ = 2.4 Hz, $J$ = 12.8 Hz, 1H), 3.96-3.87 (m, 1H), 3.49-3.30 (m, 2H), 3.23-3.05 (m, 1H), 2.92-2.72 (m, 3H), 1.92-1.79 (m, 3H), 1.62-1.53 (m, 1H), 1.27-1.23 (m, 1H); $^{13}$C NMR (100 MHz, DMSO-$d_6$) δ ppm 170.94, 150.93, 133.64, 132.93, 132.61, 128.53, 128.41, 128.04, 126.87, 126.39, 124.73, 124.57, 103.63, 52.13, 49.23, 40.63, 34.93, 27.94, 23.99; HRMS-ESI: calcd. for $C_{19}H_{22}N_3S$ $[M + H]^+$: 324.1529, found: 324.1525.

***1-(4-(6-Chloronaphthalen-2-yl)thiazol-2-yl)-4-methylpiperidin-4-amine (20)***. The title compound was prepared from **45** and 2-(6-chloronaphthalen-2-yl)-4,4,5,5-tetramethyl-1,3,2-dioxaborolane following general procedure B. White solid (111 mg, 62% yield). $^{1}$H NMR (400 MHz, $CD_3OD$) δ ppm 8.29 (s, 1H), 7.91- 7.73 (m, 4H), 7.56 (s, 2H), 7.39 (d, J = 8.0 Hz, 1H), 7.02 (s, 1H), 4.00-3.89 (m, 2H), 3.46 – 3.31 (m, 2H), 2.01 – 1.85 (m, 4H), 1.47 (s, 3H); $^{13}$C NMR (100 MHz, DMSO-$d_6$) δ ppm 170.12, 150.19, 133.08, 132.59, 131.56, 130.38, 130.26, 127.35, 126.89, 126.23, 125.27, 124.13, 103.92, 50.95, 44.28, 34.49, 23.44; HRMS-ESI: calcd. for $C_{19}H_{21}N_3ClS$ $[M + H]^+$: 358.1139, found: 358.1137.

***1-(4-(6-Fluoronaphthalen-2-yl)thiazol-2-yl)-4-methylpiperidin-4-amine (21).*** The title compound was prepared from **45** and 2-(6-fluoronaphthalen-2-yl)-4,4,5,5-tetramethyl-1,3,2-dioxaborolane following general procedure B. White solid (116 mg, 68% yield). $^{1}$H NMR (400 MHz, DMSO-$d_6$) δ ppm 8.44 (s, 1H), 8.44 (s, 1H), 8.38 (s, 2H), 8.05-8.02 (m, 2H), 7.91 (d, *J* = 8.8 Hz, 1H), 7.70 (dd, *J* = 2.0 Hz, *J* = 10.0 Hz,1H), 7.43-7.40 (m, 2H), 3.89-3.84 (m, 2H), 3.45-3.40 (m, 2H), 1.95-1.90 (m, 2H), 1.83-1.80 (m, 2H), 1.40 (s, 3H) ; $^{19}$F-NMR: -114.43 to -114.49; $^{13}$C NMR (100 MHz, DMSO-$d_6$) δ ppm 170.07, 160.03 (d, *J* = 242.4 Hz), 150.31, 133.16 (d, *J* = 9.4 Hz), 131.62 (d, *J* = 2.6 Hz), 130.98 (d, *J* = 9.0 Hz), 130.33, 127.51 (d, *J* = 5.3 Hz), 125.19, 124.29, 116.53 (d, *J* = 25.0 Hz), 110.72 (d, *J* = 20.6 Hz), 103.54, 51.83, 44.10, 33.71, 21.98; HRMS-ESI: calcd. for $C_{19}H_{21}FN_3S$ $[M + H]^+$: 342.1435, found: 342.1437.

***1-(4-(6-Methoxynaphthalen-2-yl)thiazol-2-yl)-4-methylpiperidin-4-amine (22).*** The title compound was prepared from **45** and 2-(6-Methoxynaphthalen-2-yl)-4,4,5,5-tetramethyl-1,3,2-dioxaborolane following general procedure B. White solid (104 mg, 59% yield). $^{1}$H NMR (400 MHz, DMSO-$d_6$) δ ppm 8.31 (s, 1H), 7.94 (dd, *J* = 1.6 Hz, *J* = 8.8 Hz, 2H), 7.86-7.80 (m, 2H), 7.33 (s, 1H), 7.31 (d, J = 2.4 Hz, 1H), 7.16 (dd, *J* = 2.4 Hz, *J* = 8.8 Hz, 1H), 3.88 (s, 3H), 3.84-

3.79 (m, 2H), 3.50 – 3.37 (m, 2H), 1.89 – 1.76 (m, 4H), 1.36 (s, 3H); $^{13}$C NMR (100 MHz, DMSO-$d_6$) δ ppm 170.00, 157.39, 150.77, 133.78, 130.01, 129.63, 128.48, 126.90, 124.55, 124.18, 118.89, 106.03, 102.40, 55.22, 51.28, 44.24, 34.22, 22.89; HRMS-ESI: calcd. for $C_{20}H_{24}N_3OS$ $[M + H]^+$: 354.1635, found: 354.1630.

***1-(4-(6-Bromonaphthalen-2-yl)thiazol-2-yl)-4-methylpiperidin-4-amine (23).*** Compound **42** was treated with trifluoroacetic acid and to get compound **23**. White solid (174 mg, 87% yield). $^1$H NMR (400 MHz, DMSO-$d_6$) δ ppm 8.41 (s, 1H), 8.18 (s, 1H), 8.13 (s, 2H), 8.05 (d, J = 8.8 Hz, 1H), 7.91 (d, J = 8.4 Hz, 1H), 7.62 (d, J = 8.8 Hz, 1H), 7.47 (s, 1H), 3.90-3.80 (m, 2H), 3.44 – 3.36 (m, 2H), 1.90 – 1.80 (m, 4H), 1.39 (s, 3H); $^{13}$C NMR (100 MHz, DMSO-$d_6$) δ ppm 170.07, 150.22, 133.61, 132.65, 131.71, 130.33, 129.51, 129.41, 127.33, 125.23, 124.20, 119.07, 104.22, 51.91, 44.19, 33.67, 21.71; HRMS-ESI: calcd. for $C_{19}H_{21}N_3BrS$ $[M + H]^+$: 402.0634, found: 402.0635.

***6-(2-(4-Amino-4-methylpiperidin-1-yl)thiazol-4-yl)-2-naphthonitrile (24)***. To an oven-dried round-bottomed flask was added compound **42**（50mg, 0.1 mmol）, $Zn(CN)_2$ （14 mg, 0.15 mmol）and $Pd(PPh_3)_4$ (58 mg, 0.05 mmol), then DMF (5 mL) was added, and the reaction mixture was degassed by sparging with $N_2$(g) for 10 min, at which time it was equipped with a condenser and placed in a preheated 130 °C oil-bath. After 8 h, the reaction mixture was allowed to cool to r.t, then diluted with ethyl acetate and the reaction mixture was partitioned between ethyl acetate and water. The organic layer was washed with water and brine successively, dried over anhydrous sodium sulfate, and concentrated in vacuum. The resulting residue was purified by silica gel chromatography (dichloromethane/methanol, v/v, 99:1to 95:5) to give the desired product **24**. Yellow solid (10 mg, 29% yield). $^1$H NMR (400 MHz, DMSO-$d_6$) δ ppm 8.54 (s,

1H), 8.50 (s, 1H), 8.17 – 8.12 (m, 2H), 8.06 (d, *J* = 8.8 Hz, 1H), 7.77 (dd, *J* = 1.2 Hz, *J* = 8.4 Hz,1H), 7.55 (s, 1H), 3.70-3.65 (m, 2H), 3.56-3.39 (m, 2H), 1.66-1.64 (m, 4H), 1.22 (s, 3H) ; $^{13}$C NMR (100 MHz, DMSO-$d_6$) δ ppm 170.30, 149.81, 135.07, 134.73, 134.01, 131.28, 129.56, 128.76, 126.83, 125.74, 124.11, 119.30, 107.99, 105.12, 48.90, 44.73, 36.34, 26.94; HRMS-ESI: calcd. for $C_{20}H_{21}N_4S$ $[M + H]^+$: 349.1481, found: 349.1483.

***Methyl 6-(2-(4-amino-4-methylpiperidin-1-yl)thiazol-4-yl)-2-naphthoate (25).*** The title compound was prepared from **45** and methyl 6-(4,4,5,5-tetramethyl-1,3,2-dioxaborolan-2-yl)-2-naphthoate following general procedure B. White solid (124 mg, 65% yield). $^1$H NMR (400 MHz, DMSO-$d_6$) δ ppm 8.62 (s, 1H), 8.47 (s, 1H), 8.15 (d, *J* = 8.8 Hz, 1H), 8.10 (dd, *J* = 1.2 Hz, *J* = 8.4 Hz, 1H), 8.06-8.02 (m, 3H), 7.98 (dd, *J* = 1.6 Hz, *J* = 9.6 Hz,1H), 7.57 (s, 1H), 3.94 (s, 3H), 3.92-3.85 (m, 2H), 3.50-3.40 (m, 2H), 1.90-1.80 (m, 4H), 1.40 (s, 3H) ; $^{13}$C NMR (100 MHz, DMSO-$d_6$) δ ppm 170.08, 166.33, 150.11, 135.39, 134.42, 131.52, 130.29, 129.64, 128.64, 126.70, 125.29, 125.01, 123.95, 105.11, 52.24, 51.88, 44.18, 33.66, 21.70; HRMS-ESI: calcd. for $C_{21}H_{24}N_3O_2S$ $[M + H]^+$: 382.1584, found: 382.1583.

***6-(2-(4-Amino-4-methylpiperidin-1-yl)thiazol-4-yl)-2-naphthoic acid (26).*** To an oven-dried round-bottomed flask was added compound **25**（76 mg, 0.2 mmol）, and KOH (34 mg, 0.6 mmol), then 1,4-dioxane (3 mL) and MeOH (3 mL) was added, and the reaction mixture was degassed by sparging with $N_2$(g) for 10 min, and stirred at 70 °C for 2 h, the reaction mixture was allowed to cool to r.t, water (10 mL) was added and acified with 1N HCl to PH to 2, then diluted with ethyl acetate and the reaction mixture was partitioned between ethyl acetate and water. The organic layer was washed with water and brine successively, dried over anhydrous $Na_2SO_4$, and concentrated in vacuum. The resulting residue was purified by silica gel

chromatography (dichloromethane/methanol, v/v, 99:1to 95:5) to give the desired product **26**. Yellow solid (56 mg, 76%yield). $^{1}$H NMR (400 MHz, DMSO-$d_6$) δ ppm 13.04 (s, 1H), 8.57 (s, 1H), 8.46 (s, 1H), 8.39 (s, 2H), 8.12-8.09 (m, 2H), 8.07-7.95 (m, 2H), 7.54 (s, 1H), 3.89-3.86 (m, 2H), 3.46-3.37 (m, 2H), 1.97-1.93 (m, 2H), 1.90-1.81 (m, 2H), 1.41 (s, 3H) ; $^{13}$C NMR (100 MHz, DMSO-$d_6$) δ ppm 170.08, 167.39, 150.16, 135.24, 134.17, 131.57, 130.25, 129.54, 128.41, 127.88, 125.66, 124.84, 123.95, 104.85, 51.85, 44.11, 33.86, 21.93; HRMS-ESI: calcd. for $C_{20}H_{22}N_3O_2S$ $[M + H]^+$: 368.1427, found: 368.1423.

***(6-(2-(4-Amino-4-methylpiperidin-1-yl)thiazol-4-yl)naphthalen-2-yl)methanol (27).*** To the solution of compound **25**（76 mg, 0.2 mmol）in THF (10 mL) was added $LiAlH_4$ (1M/THF, 0.5 mL) at 0 °C, then stirred at 25 °C for 2 h, the reaction mixture was allowed to cool to r.t, $Na_2SO_4.10H_2O$ was added, then diluted with ethyl acetate and subsequently filtered with celite. After the filtrate was concentrated under reduced pressure, the resulting residue was purified by chromatography to give the desired product **27**. Yellow solid (57 mg, 81% yield). $^{1}$H NMR (400 MHz, DMSO-$d_6$) δ ppm 8.43 (s, 1H), 8.10 (s, 2H), 8.10 (dd, $J$ = 1.6 Hz, $J$ = 8.4 Hz, 1H), 8.04-7.95 (m, 3H), 8.10 (dd, $J$ = 1.6 Hz, $J$ = 8.4 Hz, 1H), 7.49 (s, 1H), 5.60 (s, 2H), 3.88-3.84 (m, 2H), 3.50-3.40 (m, 2H), 1.90-1.79 (m, 4H), 1.90-1.81 (m, 2H), 1.40 (s, 3H) ; $^{13}$C NMR (100 MHz, DMSO-$d_6$) δ ppm 170.04, 150.33, 133.15, 132.81, 132.03, 131.18, 128.73, 128.29, 128.03, 126.70, 124.67, 124.06, 104.14, 69.94, 51.92, 44.19, 33.65, 22.06; HRMS-ESI: calcd. for $C_{20}H_{24}N_3OS$ $[M + H]^+$: 354.1635, found: 354.1631.

***1-(4-([1,1'-Biphenyl]-3-yl)thiazol-2-yl)-4-methylpiperidin-4-amine (28).*** The title compound was prepared from **45** and 2-([1,1'-biphenyl]-3-yl)-4,4,5,5-tetramethyl-1,3,2-dioxaborolane following general procedure B. White solid (129 mg, 74% yield). $^{1}$H NMR (400 MHz, DMSO-

$d_6$) δ ppm 8.11 (brs, 3H), 7.86 (d, *J* = 6.8 Hz, 1H), 7.73-7.67 (m, 2H), 7.60-7.55 (m, 1H), 7.51-7.46 (m, 3H), 7.44 (s, 1H), 7.42-7.36 (m, 1H), 3.85-3.79 (m, 2H), 3.42-3.35 (m, 2H), 1.89-1.78 (m, 4H), 1.38 (s, 3H) ; $^{13}$C NMR (100 MHz, DMSO-$d_6$) δ ppm 169.98, 150.51, 140.56, 140.17, 135.26, 129.20, 128.96, 127.57, 126.82, 126.01, 124.89, 123.95, 103.36, 51.90, 44.16, 33.65, 21.68; HRMS-ESI: calcd. for $C_{21}H_{24}N_3S$ $[M + H]^+$: 350.1685, found: 350.1679.

***3'-(2-(4-Amino-4-methylpiperidin-1-yl)thiazol-4-yl)-[1,1'-biphenyl]-4-carbonitrile (29).*** The title compound was prepared from **45** and 3'-(4,4,5,5-tetramethyl-1,3,2-dioxaborolan-2-yl)-[1,1'-biphenyl]-4-carbonitrile following general procedure B. White solid (129 mg, 69% yield). $^1$H NMR (400 MHz, DMSO-$d_6$) δ ppm 8.25-8.11 (m, 3H), 8.01-7.89 (m, 5H), 7.66 (d, *J* = 8.8 Hz, 1H), 7.53 (t, *J* = 7.6 Hz, 1H), 7.48 (s, 1H), 3.83-3.80 (m, 2H), 3.53-3.39 (m, 2H), 1.89-1.78 (m, 4H), 1.38 (s, 3H) ; $^{13}$C NMR (100 MHz, DMSO-$d_6$) δ ppm 170.05, 150.19, 144.63, 138.67, 135.52, 132.91, 129.52, 127.75, 126.33, 126.17, 124.20, 118.93, 110.17, 103.76, 51.86, 44.17, 33.68, 21.68; HRMS-ESI: calcd. for $C_{22}H_{23}N_4S$ $[M + H]^+$: 375.1638, found: 375.1635.

***Methyl 3'-(2-(4-amino-4-methylpiperidin-1-yl) thiazol-4-yl)-[1, 1'-biphenyl]-4-carboxylate (30).*** The title compound was prepared from **45** and methyl 3'-(4,4,5,5-tetramethyl-1,3,2-dioxaborolan-2-yl)-[1,1'-biphenyl]-4-carboxylate following general procedure B. White solid (132 mg, 65% yield). $^1$H NMR (400 MHz, DMSO-$d_6$) δ ppm 8.22 (s, 1H), 8.06 (brs, 2H), 8.01-7.95 (m, 4H), 7.74 (d, *J* = 8.4 Hz, 2H), 7.64 (t, *J* = 8.0 Hz, 1H), 7.39 (s, 1H), 3.90 (s, 3H), 3.84-3.81 (m, 2H), 3.42-3.39 (m, 2H), 1.89-1.78 (m, 4H), 1.39 (s, 3H) ; $^{13}$C NMR (100 MHz, DMSO-$d_6$) δ ppm 170.02, 166.19, 150.10, 140.28, 137.94, 134.24, 131.37, 130.39, 129.58, 128.12, 126.95, 126.89, 126.41, 103.46, 52.31, 51.94, 44.18, 33.63, 21.66; HRMS-ESI: calcd. for $C_{23}H_{26}N_3O_2S$ $[M + H]^+$: 408.1740, found: 408.1745.

***1-(4-(4'-Fluoro-[1,1'-biphenyl]-4-yl)thiazol-2-yl)-4-methylpiperidin-4-amine (31).*** The title compound was prepared from **45** and methyl 2-(4'-fluoro-[1,1'-biphenyl]-4-yl)-4,4,5,5-tetramethyl-1,3,2-dioxaborolane following general procedure B. White solid (127 mg, 69% yield).$^{1}$H NMR (400 MHz, DMSO-$d_6$) δ ppm 8.51 (s, 3H), 7.94 (d, *J* = 8.0 Hz, 2H), 7.74-7.66 (m, 4H), 7.35-7.27 (m, 3H), 3.84-3.81 (m, 2H), 3.42-3.37 (m, 2H), 1.97-1.92 (m, 2H), 1.80-1.79 (m, 2H), 1.40 (s, 3H) ; $^{19}$F-NMR: -115.42 to -115.50; $^{13}$C NMR (100 MHz, DMSO-$d_6$) δ ppm 170.04, 161.87 (d, *J* = 242.9 Hz), 150.14, 138.00, 136.17 (d, *J* = 3.0 Hz), 133.74, 128.49 (d, *J* = 8.1 Hz), 126.72, 126.29, 116.76 (d, *J* = 21.2 Hz), 102.96, 51.70, 44.04, 33.74, 22.10; HRMS-ESI: calcd. for $C_{21}H_{23}FN_3S$ $[M + H]^+$: 368.1591, found: 368.1593.

***4'-(2-(4-Amino-4-methylpiperidin-1-yl)thiazol-4-yl)-[1,1'-biphenyl]-4-ol (32).*** The title compound was prepared from **45** and 4'-(4,4,5,5-tetramethyl-1,3,2-dioxaborolan-2-yl)-[1,1'-biphenyl]-4-ol following general procedure B. White solid (130 mg, 71% yield). $^{1}$H NMR (400 MHz, DMSO-$d_6$) δ ppm 9.60 (s, 1H), 7.88 (d, *J* = 8.4 Hz, 2H), 7.59 (d, *J* = 8.4 Hz, 2H), 7.52 (d, *J* = 8.4 Hz, 2H), 7.21 (s, 1H), 6.85 (d, *J* = 8.8 Hz, 2H), 3.57-3.49 (m, 4H), 1.57-1.47 (m, 4H), 1.10 (s, 3H) ; $^{13}$C NMR (100 MHz, DMSO-$d_6$) δ ppm 170.24, 157.21, 150.41, 139.07, 132.89, 130.42, 127.56, 126.16, 125.88, 101.60, 46.85, 45.05, 38.16, 30.44; HRMS-ESI: calcd. for $C_{21}H_{24}N_3OS$ $[M + H]^+$: 366.1635, found: 366.1631.

***4-Methyl-1-(4-(quinolin-3-yl)thiazol-2-yl)piperidin-4-amine (33)***. The title compound was prepared from **45** and quinolin-3-ylboronic acid following general procedure B. Yellow solid (115 mg, 71% yield).$^{1}$H NMR (400 MHz, DMSO-$d_6$) δ ppm 9.41 (d, *J* = 1.6 Hz, 1H), 8.72 (s, 1H), 8.02 (t, *J* = 6.8 Hz, 1H), 7.73 (t, *J* = 7.2 Hz, 1H), 7.63 – 7.48 (m, 4H), 3.84-3.81 (m, 2H), 3.50-3.35 (m, 2H), 1.87-1.75 (m, 4H), 1.35 (s, 3H) ; $^{13}$C NMR (100 MHz, DMSO-$d_6$) δ ppm

170.43, 148.86, 147.89, 146.84, 131.29, 129.32, 128.75, 128.37, 127.66, 127.09, 104.69, 50.95, 44.33, 34.49, 23.46; HRMS-ESI: calcd. for $C_{18}H_{21}N_4S$ $[M + H]^+$: 325.1481, found: 325.1479.

***1-(4-(Benzo[b]thiophen-2-yl)thiazol-2-yl)-4-methylpiperidin-4-amine (34).*** The title compound was prepared from **45** and benzo[*b*]thiophen-2-ylboronic acid following general procedure B. Yellow solid (95 mg, 58% yield). $^1$H NMR (400 MHz, DMSO-$d_6$) δ ppm 8.10 (s, 2H), 7.93-7.91 (m, 1H), 7.83-7.81 (m, 1H), 7.75 (s, 1H), 7.39 – 7.31 (m, 3H), 3.82-3.77 (m, 2H), 3.43-3.34 (m, 2H), 1.89 – 1.78 (m, 4H), 1.39 (s, 3H); $^{13}$C NMR (100 MHz, DMSO-$d_6$) δ ppm 169.98, 145.20, 140.02, 138.61, 138.57, 124.65, 124.48, 123.63, 122.43, 119.68, 103.93, 51.85, 39.94, 33.58, 21.61; HRMS-ESI: calcd. for $C_{17}H_{20}N_3S_2$ $[M + H]^+$: 330.1093, found: 330.1095.

***1-(4-(Bibenzo[b,d]furan-4-yl)thiazol-2-yl)-4-methylpiperidin-4-amine (35).*** The title compound was prepared from **45** and dibenzo[*b,d*]furan-4-ylboronic acid following general procedure B. Yellow solid (126 mg, 69% yield). $^1$H NMR (400 MHz, DMSO-$d_6$) δ ppm 8.19-8.16 (m, 2H), 8.12-8.09 (m, 3H), 7.82-7.45 (m, 2H), 7.57 (t, $J$ = 8.0 Hz, 1H), 7.49-7.43 (m, 2H), 3.89-3.85 (m, 2H), 3.47-3.37 (m, 2H), 1.92 – 1.80 (m, 4H), 1.40 (s, 3H); $^{13}$C NMR (100 MHz, DMSO-$d_6$) δ ppm 169.43, 155.40, 152.03, 145.44, 127.72, 126.06, 124.12, 123.39, 123.30, 123.12, 121.21, 120.15, 119.27, 111.84, 107.49, 51.91, 44.21, 33.65, 21.67; HRMS-ESI: calcd. for $C_{21}H_{22}N_3OS$ $[M + H]^+$: 364.1478, found: 364.1473.

***1-(Naphthalen-2-yl)-2-thiocyanatoethan-1-one (37d).*** A solution of 2-bromo-1-(naphthalen-2-yl) ethan-1-one **(36d)** (249 mg, 1.0 mmol) and potassium thiocyanate (194 mg, 2 mmol, ) in ethanol (5 mL) was stirred at 85°C for 2h. The reaction was extracted with diethyl ether and dried with $MgSO_4$, and then the solvent was removed at low pressure. The crude product was purified by chromatography to get compound **37d** (225mg, 99% yield) as white solid. $^1$H NMR

(300 MHz, $CDCl_3$) δ ppm 8.45 (s, 1H), 7.95 (dd, *J* = 20.5, 11.0 Hz, 4H), 7.65 (dt, *J* = 15.0, 6.9 Hz, 2H), 4.89 (s, 2H).

***2-Bromo-4-(naphthalen-2-yl)thiazole (38d).*** A suspension of **37d** (227 mg, 1.0 mmol) in 2 mL 30% hydrogen bromide in acetic acid and 3 mL acetic acid was stirred under nitrogen at room temperature overnight. The mixture was quenched with $Na_2CO_3$ aqueous solution, then extracted with ethyl acetate and washed with water and brine, the organic was dried with $MgSO_4$ and solvent was removed at low pressure. The crude product was purified by chromatography to get compound **38d** (261 mg, 90% yield) as white solid. $^1$H NMR (400 MHz, $CDCl_3$) δ ppm 8.43 (s, 1H), 7.93 – 7.83 (m, 4H), 7.53 – 7.49 (m, 3H).

***2-Bromo-4-(6-bromonaphthalen-2-yl)thiazole (41)***. The compound was prepared by following a procedure similar to that of **38d**. White solid (321 mg, 87%yield). $^1$H NMR (400 MHz, $CDCl_3$) δ ppm 8.51 (s, 1H), 8.32 (s, 1H), 8.23(d, *J* = 1.6 Hz , 1H), 8.09 (dd, *J* = 8.4 Hz, *J* =1.6 Hz, 1H), 8.01-7.97 (m, 2H); $^{13}$C NMR (100 MHz, DMSO-$d_6$) δ ppm 154.01, 136.53, 133.94, 131.66, 130.87, 130.65, 129.69, 129.59, 127.85, 124.92, 124.89, 119.78, 119.73.

***Tert-butyl (1-(4-(6-bromonaphthalen-2-yl)thiazol-2-yl)-4-methylpiperidin-4-yl)carbamate (42).*** The title compound was prepared from **41** and tert-butyl (4-methylpiperidin-4-yl)carbamate following general procedure A. Yellow solid (245 mg, 56% yield). $^1$H NMR (400 MHz, DMSO-$d_6$) δ ppm 8.41 (s, 1H), 8.18(d, *J* = 0.8 Hz , 1H), 8.04 (dd, *J* = 1.6 Hz, *J* = 8.8 Hz,1H), 7.94 – 7.89 (m, 2H), 7.62 (dd, *J* = 2.0 Hz, *J* = 8.8 Hz,1H), 7.43 (s, 1H), 6.68 (s, 1H), 3.68-3.64 (m, 2H), 3.34-3.28 (m, 2H), 2.18-2.15 (m, 2H), 1.59-1.52 (m, 2H), 1.39 (s, 9H), 1.27 (s, 3H) ; $^{13}$C NMR (100 MHz, DMSO-$d_6$) δ ppm 170.38, 150.18, 133.58, 132.75, 131.75, 130.39, 129.50, 129.37, 127.28, 125.24, 124.11, 119.01, 103.65, 77.49, 49.73, 44.56, 34.26, 28.32, 25.98.

***Tert-butyl (1-(4-bromothiazol-2-yl)-4-methylpiperidin-4-yl)carbamate (45)***. A mixture of 2, 4-dibromothiazole **(43)** (1.22 g, 5.0 mmol), tert-butyl (4-methylpiperidin-4-yl)carbamate **(44)** (1.61 g, 7.5 mmol) in DMF ( 50 mL) and TEA ( 3.0 mL, 15 mmol) was heated to 90 °C for 8 h. The reaction mixture was cooled to room temperature, diluted with water and extracted with ethyl acetate and washed with water and brine, the organic was dried with $MgSO_4$ and solvent was removed at low pressure. The crude product was purified by chromatography to get compound 7 (1.65 g, 87%) as light yellow solid. $^1$H NMR (400 MHz, DMSO-$d_6$) δ ppm 6.84 (s, 1H), 6.66 (s, 1H), 3.51-3.41 (m, 2H), 3.24-3.17 (m, 2H), 2.11-2.08 (m, 2H), 1.52-1.45 (m, 2H), 1.38 (s, 9H), 1.24(s, 3H); $^{13}$C NMR (100 MHz, DMSO-$d_6$) δ ppm 170.18, 154.51, 120.57, 104.23, 77.51, 56.06, 49.59, 44.15, 34.07, 28.31

**Biological Evaluation. SHP2 protein expression and purification.** Genes encoding $SHP2^{WT}$, $SHP2^{E76A}$, $SHP2^{C459S}$ and $SHP2^{PTP}$ were inserted into pET28a. These constructs were used to transform BL21(DE3) competent cells and cultured at 37 $^oC$ in Luria broth(LB). When $OD_{600}$ reached 0.6, 0.5 mM IPTG was added to induce SHP2 protein expression for 5 hours at 30 $^oC$. Cells were collected by centrifugation (4500rpm 15min) and resuspended in lysis buffer containing 20 mM Tris-HCl (pH7.5), 500 mM NaCl and 0.1 mM PMSF. After the cell lysis by ultrasonication, cell lysates were centrifuged at 4 $^oC$ for 40min at 16000rpm. Then the supernatants were loaded onto HisTrap HP column, and gradient eluted by 25, 50,100, 250 mM imidazole. Eluents containing SHP2 protein were further loaded onto HiLoad Superdex 200PG column. Fractions were collected according to the results of SDS-PAGE and then concentrated the protein to 10 mg/ml or more.

***In vitro* phosphatase assay.** Artificial substrate 6,8-difluoro-4-methylumbelliferyl phosphate (DIFMUP) (Invitrogen) was used to examine the catalytic activity of phosphatases. Reactions

were performed at room temperature in 96-well black polystyrene plate with a final volume of 100μL. The $SHP2^{E76A}$ enzyme (1.5nM) and various concentrations of compounds were pre-incubated for 20min (buffer condition: 0.1M sodium acetate, pH 5.0), then added the substrate DIFMUP, incubated another 20min, and measured EX/EM 358/455. For selectivity study, different phosphatases including LmwPTP, MKP3, PTP1B, TC-PTP, SHP1, VHR and CDC25A were purified from *E.coli* and measured as the same condition as $SHP2^{E76A}$, with the exception of the DIFMUP concentration corresponding to their respective Km value. For $IC_{50}$ determination, eight concentrations of compounds at 3-fold dilution were tested. Each experiment was performed in duplicate, and $IC_{50}$ data were derived from at least three independent experiments. The curve fitting program Prism 4 (GraphPad Software) was used to calculate the $IC_{50}$ value.

**Immunoblot analysis.** NCI-H661 cells were cultured in 6-well plate, and treated with SHP2 inhibitors for 2h at 37 $^{o}$C. Cells were lysed with RIPA buffer. After centrifugation at 4 $^{o}$C for 30min at 12000rpm, 3 volumes of protein extracts were mixed with 1 volume of 4× loading buffer and loaded onto the SDS-PAGE gel. Proteins were then transferred to PVDF membranes (Millipore), blocked with 5% non-fat milk, and incubated with pERK1/2, ERK1/2, pAKT and AKT (Cell Signaling Technology) and other antibodies overnight at 4 $^{o}$C. Corresponding secondary antibodies were applied and further detected using Amersham Imager 600. The results have been repeated for at least three times.

**Immunofluorescence cell staining.** NCI-H1975 cells were seeded in 24-well plate with a coverslip in each well and grown overnight. After the treatment of 10 μM SHP2 inhibitor for 2 hours, aspirated the medium and fixed the cells with 4% PFA. Treated the coverslip with 0.4% Triton X-100 and blocked with 5% BSA. Diluted phospho-ERK1/2 antibody (Cell Signaling

Technology) was applied to the coverslip and incubated overnight at 4 °C. After PBS washing, corresponding fluorochrome-labeled secondary antibody was applied at room temperature for 1h and further PBS washed. After mounting with DAPI, examined the slides under the fluorescence microscope. The results have been repeated for at least three times.

**Luciferase reporter assay.** SF268 cells stably expressing Yap-Luc reporter were plated out onto 96-well plate in RPMI-1640. On day 1, SHP2 inhibitors at the concentrations of 3, 6 and 12μM were added. 12 hours later, cells in each well were lysed and used to measure Renilla luciferase (Promega) and CellTiter-Glo (Promega), respectively. Luciferase of the Yap reporter was normalized by the luciferase of CellTiter-Glo.

**RT-PCR experiments.** RNA was extracted from SF268 cells treated with DMSO, 10μM and 20 μM SHP2 inhibitor for 2h and then performed cDNA synthesis. Quantstudio 6 Flex was used to conduct quantitative PCR(qPCR) analysis and the primer pairs used were as follows:

| Gene (human) | Forward primer | Reverse primer |
|---|---|---|
| CTGF | 5'-GAAGCTGACCTGGAAGAGAACA -3' | 5'-CGTCGGTACATACTCCACAGAA -3' |
| ANKRD1 | 5’-AAACATCCAGGTTTCCTCCA-3’ | 5’-TTTGGCAATTGTGGAGAAGTTA-3’ |
| YAP1 | 5’-GCAAATTCTCCAAAATGTCAGG-3’ | 5’-CGGGAGAAGACACTGGATTT-3’ |
| GAPDH | 5'-GCAAATTCCATGGCACCGT-3' | 5'-TCGCCCCACTTGATTTTGG-3' |

**Cell proliferation assay.** Cells (3000 cells/well) of each cell line were seeded in 96-well plates and grown overnight. The cells were treated with SHP2 inhibitors at indicated concentrations for 2 days. Cell viability was examined by CellTiter-Glo (Promega).

**Soft agar assay.** Soft agar assay was performed in 6-well plate and consisted of two layers. The bottom layer was filled with 2 mL 1% low melting temperature agarose. In the top layer, cells were re-suspended in media containing 0.4% agarose and seeded at 10,000 cells per well in a volume of 2mL. Varying concentrations of SHP2 inhibitors were applied and supplemented 3-5 drops twice a week. 2 weeks later, colonies were stained with iodonitrotetrazolium chloride (Sigma) and visualized with Gel Imager (Bio-Rad).

***In vitro* dephosphorylation.** YAP Y357 peptide (SGLSMSSYSVPRTPD) and pY 357 peptide (SGLSMSSpYSVPRTPD) were synthesized to perform *in vitro* dephosphorylation experiments with purified $SHP2^{E76A}$ protein. The $SHP2^{E76A}$ enzyme (1.5nM) and 20μM **23** were pre-incubated for 15min (buffer condition: 20mM Tris-HCl pH 7.4, 100mM NaCl, 1mM EDTA, 2mM DTT), then added the substrate 100μM pY357 peptide, incubated another 15min. The reactions were stopped by separating the $SHP2^{E76A}$ phosphatase from the mixture using 30KD filters and then analyzed the results using p-YAP(Y357) antibody (Abcam).

**Dot blot.** 2μL of the reaction products from *in vitro* dephosphorylation experiments were loaded onto nitrocellulose membrane using narrow-mouth pipette tip and let the membrane dry. Block non-specific sites by soaking in 5% BSA in TBST for 1h, then diluted (1:1000) p-YAP(Y357) antibody (Abcam) can be applied for 1h at room temperature. After 3 times of TBST washing, secondary antibody was incubated. Another 3 times of TBST washing, incubate ECL reagent for 1minute, cover with Saran-wrap, and expose X-ray film in the dark room.

**Crystallization and X-ray data collection.** Hanging drop vapor diffusion was applied to crystalize $SHP2^{E76A}$(1-534). The reservoir solution consisted of 0.2 M Sodium formate, 0.1 M Bicine pH8.5 and 15% w/v PEG 5000MME. 1 μL $SHP2^{E76A}$ (1-534) (8.8mg/ml) was mixed with

2μL reservoir solution. Crystal appeared about 3 days at 18 $^{o}$C, and then soaked in the crystallization solution with different concentrations of SHP2 inhibitors. To obtain X-ray data, crystals were transferred into cryoprotection buffer containing crystallization solution added with 20% glycerol and then flash-cooled by liquid nitrogen. X-ray data were collected at BL19U1 beamline at Shanghai Synchrotron Radiation Facility. Data were processed using the XDS/XSCALE program[44].

**Structure determination and refinements.** Experimental phases were obtained by molecular replacement using the program Phaser[45] with a structural model of SHP2 (PDB code: 2SHP). Crystallographic refinements were performed with the program PHENIX[46]. Model building was performed using COOT[47, 48]. Data processing and refinement statistics are reported in Table 1.

**Pharmacokinetics.** During the study, the care and use of animals will be conducted in accordance with the regulations of the Association for Assessment and Accreditation of Laboratory Animal Care (AAALAC), laboratory animal administration in China and the Guide for the Care and Use of Laboratory Animals. Female nu/nu nude mice were obtained from Shanghai SLAC Laboratory Animal Co., LTD. Following IV administration (via tail vein) at 5 mg/kg, approximately 50 μL of whole blood was collected from the eyes and heart at 0.083, 0.25, 0.5, 1, 2, 4, 8 and 24h post-dose. Non-terminal blood samples were taken via orbital sinus vein puncture and study end blood samples were taken via cardiac puncture with EDTA-2K as anticoagulant. Oral administration (10 mg/kg) and collection procedures were same to IV. The blood was centrifuged at 5000 rpm, 4 $^{o}$C for 15min and plasma was transferred to Eppendorf tube and stored frozen. Samples were precipitated and diluted with acetonitrile containing internal standard and prepared for LC/MS/MS. 20μL of each sample was injected into an API4000 LC/MS/MS system for analysis, and transitions of 352.05 amu (Q1) and 267.10 amu

(Q3) were monitored. Noncompartmental analyses were used to obtain the pharmacokinetic parameters here and all the calculations derived from the computer program WinNonlin (Version 6.4).

**Tumor Xenograft Experiments.** During the study, the care and use of animals will be conducted in accordance with the regulations of the Association for Assessment and Accreditation of Laboratory Animal Care (AAALAC), laboratory animal administration in China and the Guide for the Care and Use of Laboratory Animals. Female BALB/c nude mice were inoculated subcutaneously (5 x $10^6$ cells) in a suspension containing 50% phenol red-free matrigel (BD Biosciences) in PBS with MV4;11 cells. In efficacy studies, mice were measured twice a week by calipering in two dimensions. When tumors reached roughly 230 $mm^3$, mice were randomly assigned to three treatment groups: vehicle, 10 and 30 (mg/kg, 10ml/kg, qd) by oral gavage. Tumor volume and mouse body weight were assessed twice weekly.

## ANCILLARY INFORMATION

*Supporting information* is available which includes additional pharmacology results and NMR spectra for final compounds.

*PDB ID Codes*: 5XZR for SHP2 in complex with compound **10**. Authors will release the atomic coordinates and experimental data upon article publication.

## AUTHOR INFORMATION

### Corresponding Author

*To whom correspondence should be addressed. Email address: zhujd@sioc.ac.cn (J. Zhu), liulab@sioc.ac.cn (C. Liu)

**Author Contributions**

J. X., X. S., and J. Z. designed research; J. X., X. S., S. G., and H. L. performed research; S. G., J. S., M. W., and J. S. contributed new reagents/analytic tools; D.L. helped to refine the structure and J. X., Y. F., C. L. and J. Z. analyzed data; and J. X, X. S., M. W., and J. Z. wrote the paper.

#These authors contributed equally.

**Funding Sources**

This work was supported by the “100 Talents” Program of Chinese Academy of Sciences, the "Personalized Medicines-Molecular Signature-based Drug Discovery and Development" Strategic Priority Research Program of the Chinese Academy of Sciences (Grant No. XDA12000000), Shanghai Municipal Committee of Science and Technology (No: 14ZR1448600, 15ZR1449000), a State High-Tech Development Plan (the "863 Program") Award (grand 2015AA020907), and The National Key Research and Development Program (2016YFA0501900).

**Notes**

The authors declare no competing financial interest.

**ACKNOWLEDGMENTS**

We thank Prof. Jiahai Zhou and Prof. Lifeng Pan (Shanghai Institute of Organic Chemistry) for helpful discussions on protein purification and crystallization.

**ABBREVIATIONS USED**

PTP, protein tyrosine phosphatase; RAS, rat sarcoma protein; AKT, protein kinase B; MAPK, mitogen-activated protein kinases; ERK, extracellular signal-regulated kinases; YAP, Yes associated protein; FLT3-ITD, FMS-like tyrosine kinase 3 – internal tandem duplications.

## REFERENCES

(1) Tonks, N. K. Protein tyrosine phosphatases: from genes, to function, to disease. *Nature Reviews Molecular Cell Biology*. **2006,** *7*, 833-846.

(2) Huijsduijnen, R. H. V.; Bombrun, A.; Swinnen, D. Selecting protein tyrosine phosphatases as drug targets. *Drug Discovery Today*. **2002,** *7*, 1013-1019.

(3) Li, L.; Dixon, J. E. Form, function, and regulation of protein tyrosine phosphatases and their involvement in human diseases ☆. *Semin. Immunol.* **2000,** *12*, 75-84.

(4) Zhang, Z. Y. Protein tyrosine phosphatases: prospects for therapeutics. *Curr. Opin. Chem. Biol.* **2001,** *5*, 416-423.

(5) Bialy, L.; Waldmann, H. Inhibitors of protein tyrosine phosphatases: next-generation drugs? *Angew. Chem. Int. Ed.* **2005,** *44*, 3814-3839.

(6) Mohi, M. G.; Neel, B. G. The role of Shp2 (PTPN11) in cancer. *Curr. Opin. Genet. Dev.* **2007,** *17*, 23-30.

(7) Chan, R. J.; Feng, G. S. PTPN11 is the first identified proto-oncogene that encodes a tyrosine phosphatase. *Blood*. **2007,** *109*, 862-867.

(8) Matozaki, T.; Murata, Y.; Saito, Y.; Okazawa, H.; Ohnishi, H. Protein tyrosine phosphatase

SHP-2: a proto-oncogene product that promotes Ras activation. *Cancer Sci.* **2009,** *100*, 1786-1793.

(9) Hanafusa, H.; Torii, S.; Yasunaga, T.; Nishida, E. Sprouty1 and Sprouty2 provide a control mechanism for the Ras/MAPK signalling pathway. *Nat. Cell Biol.* **2002,** *4*, 850-858.

(10) Ren, Y.; Meng, S.; Mei, L.; Zhao, Z. J.; Jove, R.; Wu, J. Roles of Gab1 and SHP2 in paxillin tyrosine dephosphorylation and Src activation in response to epidermal growth factor. *J. Biol. Chem.* **2004,** *279*, 8497-8505.

(11) Montagner, A.; Perret, B.; Yart, A.; Dance, M.; Salles, J. P.; Raynal, P. A novel role for Gab1 and SHP2 in epidermal growth factor-induced Ras activation. *J. Biol. Chem.* **2005,** *280*, 5350-5360.

(12) Agazie, Y. M.; Hayman, M. J. Molecular mechanism for a role of SHP2 in epidermal growth factor receptor signaling. *Mol. Cell. Biol.* **2003,** *23*, 7875-7886.

(13) Kawabuchi, M.; Satomi, Y.; Takao, T.; Shimonishi, Y.; Nada, S.; Nagai, K.; Tarakhovsky, A.; Okada, M. Transmembrane phosphoprotein Cbp regulates the activities of Src-family tyrosine kinases. *Nature*. **2000,** *404*, 999-1003.

(14) Hof, P.; Pluskey, S.; Dhe-Paganon, S.; Eck, M. J.; Shoelson, S. E. Crystal structure of the tyrosine phosphatase SHP-2. *Cell*. **1998,** *92*, 441-450.

(15) Tartaglia, M.; Mehler, E. L.; Goldberg, R.; Zampino, G.; Brunner, H. G.; Kremer, H.; Burgt, I. V. D.; Crosby, A. H.; Ion, A.; Jeffery, S. Mutations in the protein tyrosine kinase gene, PTPN11, cause Noonan syndrome. *Nat. Genet.* **2001,** *29*, 491-491.

(16) Bentiresalj, M.; Paez, J. G.; David, F. S.; Keilhack, H.; Halmos, B.; Naoki, K.; Maris, J. M.; Richardson, A.; Bardelli, A.; Sugarbaker, D. J. Activating mutations of the noonan syndrome-associated SHP2/PTPN11 gene in human solid tumors and adult acute myelogenous leukemia.

*Cancer Res.* **2004,** *64*, 8816-8820.

(17) Miyamoto, D.; Miyamoto, M.; Takahashi, A.; Yomogita, Y.; Higashi, H.; Kondo, S.; Hatakeyama, M. Isolation of a distinct class of gain-of-function SHP-2 mutants with oncogenic RAS-like transforming activity from solid tumors. *Oncogene*. **2008,** *27*, 3508–3515.

(18) Chan, G.; Kalaitzidis, D.; Neel, B. G. The tyrosine phosphatase Shp2 (PTPN11) in cancer. *Cancer Metastasis Rev.* **2008,** *27*, 179-192.

(19) Hatakeyama, M.; Higashi, H. Helicobacter pylori CagA: a new paradigm for bacterial carcinogenesis. *Cancer Sci.* **2005,** *96*, 835-843.

(20) Aceto, N.; Sausgruber, N.; Brinkhaus, H.; Gaidatzis, D.; Martinybaron, G.; Mazzarol, G.; Confalonieri, S.; Quarto, M.; Hu, G.; Balwierz, P. J. Tyrosine phosphatase SHP2 promotes breast cancer progression and maintains tumor-initiating cells via activation of key transcription factors and a positive feedback signaling loop. *Nat. Med.* **2012,** *18*, 529-537.

(21) Tsutsumi, R.; Masoudi, M.; Takahashi, A.; Fujii, Y.; Hayashi, T.; Kikuchi, I.; Satou, Y.; Taira, M.; Hatakeyama, M. YAP and TAZ, Hippo signaling targets, act as a rheostat for nuclear SHP2 function. *Dev. Cell*. **2013,** *26*, 658–665.

(22) Gavrieli, M.; Watanabe, N.; Loftin, S. K.; Murphy, T. L.; Murphy, K. M. Characterization of phosphotyrosine binding motifs in the cytoplasmic domain of B and T lymphocyte attenuator required for association with protein tyrosine phosphatases SHP-1 and SHP-2. *Biochem. Biophys. Res. Commun.* **2003,** *312*, 1236-1243.

(23) Yokosuka, T.; Takamatsu, M.; Kobayashiimanishi, W.; Hashimototane, A.; Azuma, M.; Saito, T. Programmed cell death 1 forms negative costimulatory microclusters that directly inhibit T cell receptor signaling by recruiting phosphatase SHP2. *J. Exp. Med.* **2012,** *209*, 1201-1217.

(24) Chemnitz, J. M.; Parry, R. V.; Nichols, K. E.; June, C. H.; Riley, J. L. SHP-1 and SHP-2 associate with immunoreceptor tyrosine-based switch motif of programmed death 1 upon primary human T cell stimulation, but only receptor ligation prevents T cell activation. *J. Immunol.* **2004,** *173*, 945-954.

(25) Butterworth, S.; Overduin, M.; Barr, A. J. Targeting protein tyrosine phosphatase SHP2 for therapeutic intervention. *Future Med. Chem.* **2014,** *6*, 1423-1437.

(26) Lawrence, H. R.; Pireddu, R.; Chen, L.; Luo, Y.; Sung, S. S.; Szymanski, A. M.; Yip, M. L.; Guida, W. C.; Sebti, S. M.; Wu, J. Inhibitors of Src homology-2 domain containing protein tyrosine phosphatase-2 (Shp2) based on oxindole scaffolds. *J. Med. Chem.* **2008,** *51*, 4948-4956.

(27) Zeng, L. F.; Zhang, R. Y.; Yu, Z. H.; Li, S.; Wu, L.; Gunawan, A. M.; Lane, B. S.; Mali, R. S.; Li, X.; Chan, R. J. Therapeutic potential of targeting the oncogenic SHP2 phosphatase. *J. Med. Chem.* **2014,** *57*, 6594-6609.

(28) Chen, L.; Sung, S. S.; Yip, M. L.; Lawrence, H. R.; Ren, Y.; Guida, W. C.; Sebti, S. M.; Lawrence, N. J.; Wu, J. Discovery of a novel shp2 protein tyrosine phosphatase inhibitor. *Mol. Pharmacol.* **2006,** *70*, 562-570.

(29) Nören-Müller, A.; Reis-Corrêa, I.; Prinz, H.; Rosenbaum, C.; Saxena, K.; Schwalbe, H. J.; Vestweber, D.; Cagna, G.; Schunk, S.; Schwarz, O. Discovery of protein phosphatase inhibitor classes by biology-oriented synthesis. *Proc. Natl. Acad. Sci. U. S. A.* **2006,** *103*, 10606-10611.

(30) Hellmuth, K.; Grosskopf, S.; Lum, C. T.; Würtele, M.; Röder, N.; Kries, J. P. V.; Rosario, M.; Rademann, J.; Birchmeier, W. Specific inhibitors of the protein tyrosine phosphatase Shp2 identified by high-throughput docking. *Proc. Natl. Acad. Sci. U. S. A.* **2008,** *105*, 7275-7280.

(31) Zhang, X.; He, Y.; Liu, S.; Yu, Z.; Jiang, Z. X.; Yang, Z.; Dong, Y.; Nabinger, S. C.; Wu, L.; Gunawan, A. M. Salicylic acid based small molecule inhibitor for the oncogenic Src homology-2

domain containing protein tyrosine phosphatase-2 (SHP2). *J. Med. Chem.* **2010,** *53*, 2482-2493.

(32) Liu, W.; Yu, B.; Xu, G.; Xu, W. R.; Loh, M. L.; Tang, L. D.; Qu, C. K. Identification of Cryptotanshinone as an inhibitor of oncogenic protein tyrosine phosphatase SHP2 (PTPN11). *J. Med. Chem.* **2013,** *56*, 7212-7221.

(33) Chen, Y. N. P.; Lamarche, M. J.; Chan, H. M.; Fekkes, P.; Garciafortanet, J.; Acker, M. G.; Antonakos, B.; Chen, H. T.; Chen, Z.; Cooke, V. G. Allosteric inhibition of SHP2 phosphatase inhibits cancers driven by receptor tyrosine kinases. *Nature*. **2016**, *535*, 148-152

(34) Garcia, F. J.; Chen, C. H.; Chen, Y. P.; Chen, Z.; Deng, Z.; Firestone, B.; Fekkes, P.; Fodor, M.; Fortin, P. D.; Fridrich, C. Allosteric inhibition of SHP2: identification of a potent, selective, and orally efficacious phosphatase inhibitor. *J. Med. Chem.* **2016**, *59*, 7773-7782

(35) Krishnan, N.; Koveal, D.; Miller, D. H.; Xue, B.; Akshinthala, S. D.; Kragelj, J.; Jensen, M. R.; Gauss, C. M.; Page, R.; Blackledge, M. Targeting the disordered C terminus of PTP1B with an allosteric inhibitor. *Nat. Chem. Biol.* **2014,** *10*, 558-566.

(36) Gilmartin, A. G.; Faitg, T. H.; Richter, M.; Groy, A.; Seefeld, M. A.; Darcy, M. G.; Peng, X.; Federowicz, K.; Yang, J.; Zhang, S. Y. Allosteric Wip1 phosphatase inhibition through flap-subdomain interaction. *Nat. Chem. Biol.* **2014,** *10*, 181-187.

(37) Larochelle, J. R.; Fodor, M.; Xiang, X.; Durzynska, I.; Fan, L.; Stams, T.; Chan, H.; Lamarche, M. J.; Chopra, R.; Ping, W. Structural and functional consequences of three cancer-associated mutations of the oncogenic phosphatase SHP2. *Biochemistry*. **2016,** *55*, 2269-2277

(38) Hanafusa, H.; Torii, S.; Yasunaga, T.; Matsumoto, K.; Nishida, E. Shp2, an SH2-containing protein-tyrosine phosphatase, positively regulates receptor tyrosine kinase signaling by dephosphorylating and inactivating the inhibitor Sprouty. *J. Biol. Chem.* **2004,** *279*, 22992-22995.

(39) Keilhack, H.; David, F. S.; Mcgregor, M.; Cantley, L. C.; Neel, B. G. Diverse biochemical properties of Shp2 mutants. Implications for disease phenotypes. *J. Biol. Chem.* **2005,** *280*, 30984-30993.

(40) Wang, W.; Liu, L.; Song, X.; Mo, Y.; Komma, C.; Bellamy, H. D.; Zhao, Z. J.; Zhou, G. W. Crystal structure of human protein tyrosine phosphatase SHP-1 in the open conformation. *J. Cell. Biochem.* **2011,** *112*, 2062-2071.

(41) Xu, J.; Zeng, L. F.; Shen, W.; Turchi, J. J.; Zhang, Z. Y. Targeting SHP2 for EGFR inhibitor resistant non-small cell lung carcinoma. *Biochem. Biophys. Res. Commun.* **2013,** *439*, 586-590.

(42) Stein, C.; Bardet, A. F.; Roma, G.; Bergling, S.; Clay, I.; Ruchti, A.; Agarinis, C.; Schmelzle, T.; Bouwmeester, T.; Schübeler, D. YAP1 exerts its transcriptional control via TEAD-mediated activation of enhancers. *PLoS Genet.* **2015,** *11*, e1005465.

(43) Keshet, R.; Adler, J.; Ricardo, L. I.; Shanzer, M.; Porat, Z.; Reuven, N.; Shaul, Y. C-Abl antagonizes the YAP oncogenic function. *Cell Death Differ.* **2014,** *22*, 935-945.

(44) Kabsch, W. Automatic processing of rotation diffraction data from crystals of initially unknown symmetry and cell constants. *J. Appl. Crystallogr.* **1993,** *26*, 795–800.

(45) Mccoy, A. J.; Grossekunstleve, R. W.; Storoni, L. C.; Read, R. J. Likelihood-enhanced fast translation functions. *Acta Crystallogr.* **2005,** *61*, 458–464.

(46) Adams, P. D.; Afonine, P. V.; Bunkóczi, G.; Chen, V. B.; Davis, I. W.; Echols, N.; Headd, J. J.; Hung, L. W.; Kapral, G. J.; Grossekunstleve, R. W. PHENIX: a comprehensive Python-based system for macromolecular structure solution. *Acta Crystallogr.* **2009,** *66*, 213-221.

(47) Emsley, P.; Cowtan, K. Coot : model-building tools for molecular graphics. *Acta Crystallogr.* **2005,** *60*, 2126-2132.

(48) Krissinel, E. B.; Winn, M. D.; Ballard, C. C.; Ashton, A. W.; Patel, P.; Potterton, E. A.;

Mcnicholas, S. J.; Cowtan, K. D.; Emsley, P. The new CCP4 Coordinate Library as a toolkit for the design of coordinate-related applications in protein crystallography. *Acta Crystallogr.* **2004,** *60*, 2250.

(49) Commons, T. J.; Fensome, A.; Heffernan, G. D.; McComas, C. C.; Woodworth, R. P.; Webb, M. B.; Marella, M. A.; Melenski, E. G. Pyrrolidine and Related Derivatives Useful as PR Modulators. WO2008021339, 2008.

## FIGURES

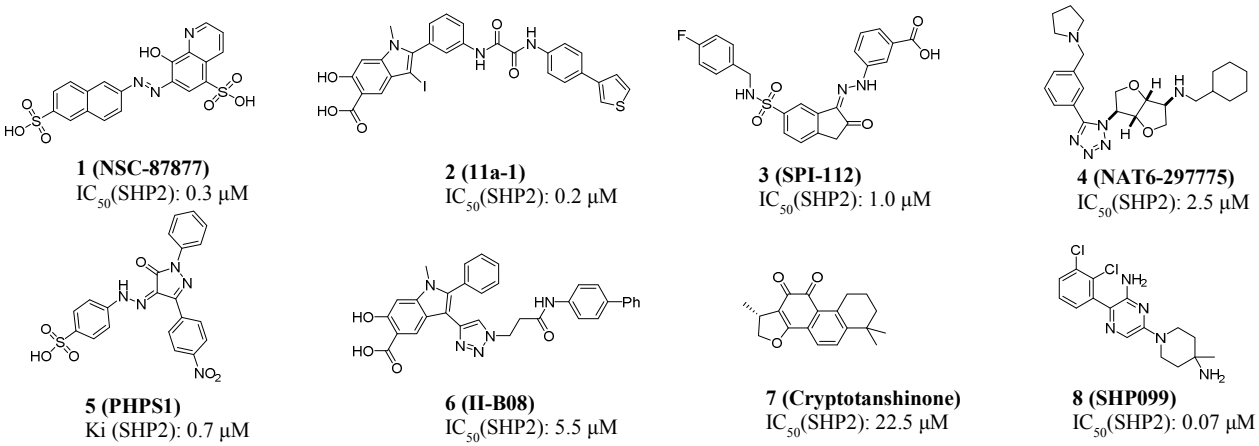


**Figure 1.** Representative known SHP2 inhibitors.

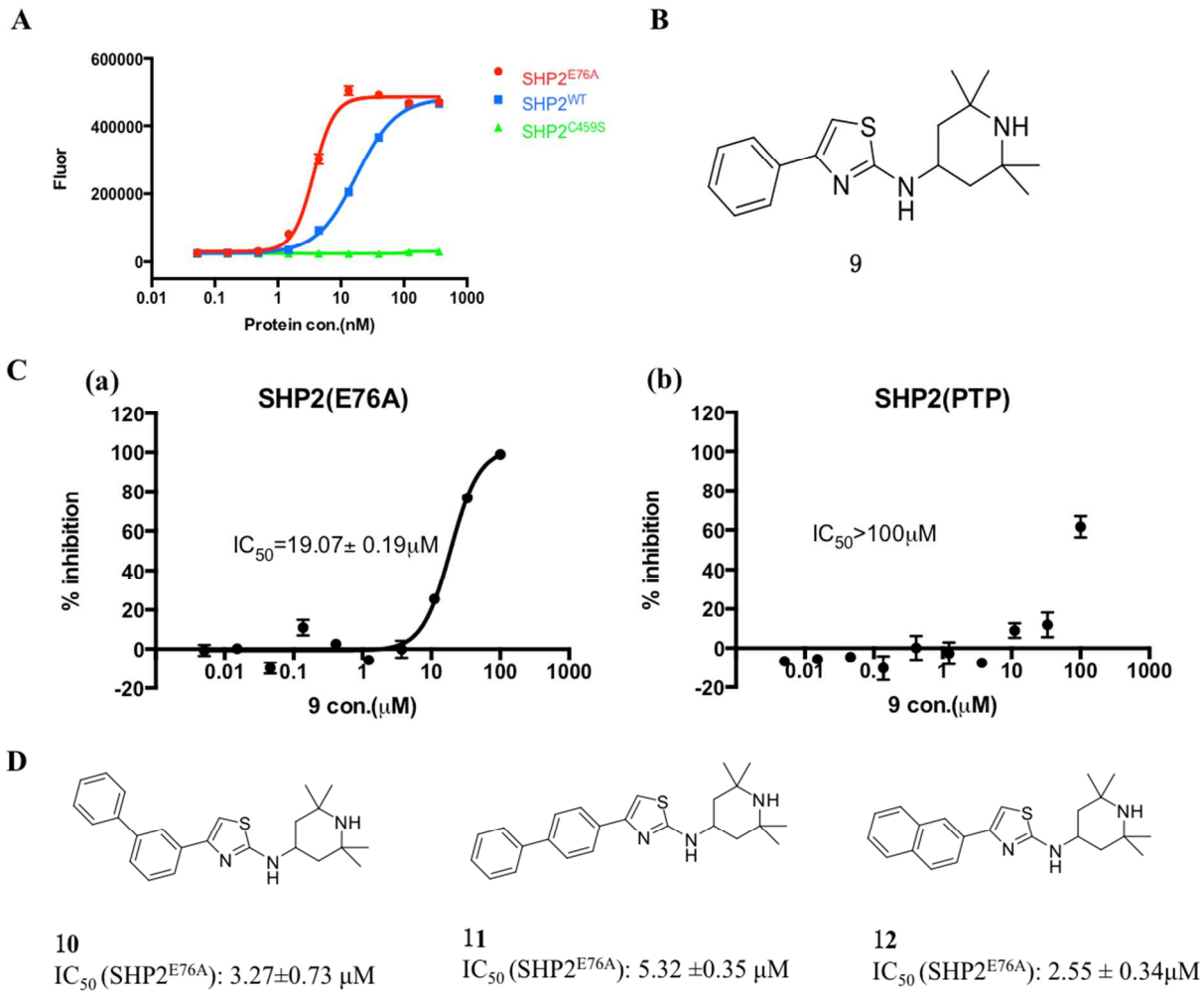


**Figure 2.** Identification of SHP2 inhibitors through $SHP2^{E76A}$ biochemical screening. **A.** Catalytic activity of purified $SHP2^{E76A}$, $SHP2^{WT}$ and $SHP2^{C459S}$. Phosphatase assays were conducted using the artificial substrate DIFMUP, and data represents mean±s.d.(n=3); **B.** Structure of **9**; **C.** Compound **9** inhibited $SHP2^{E76A}$ with moderate potency(**a**) but had no effect on $SHP2^{PTP}$(**b**). Data represents mean±s.d.(n=3); **D.** Structures and $IC_{50}$s of **10**, **11**, and **12**. Each IC50 is at least the mean of 3 determinations.

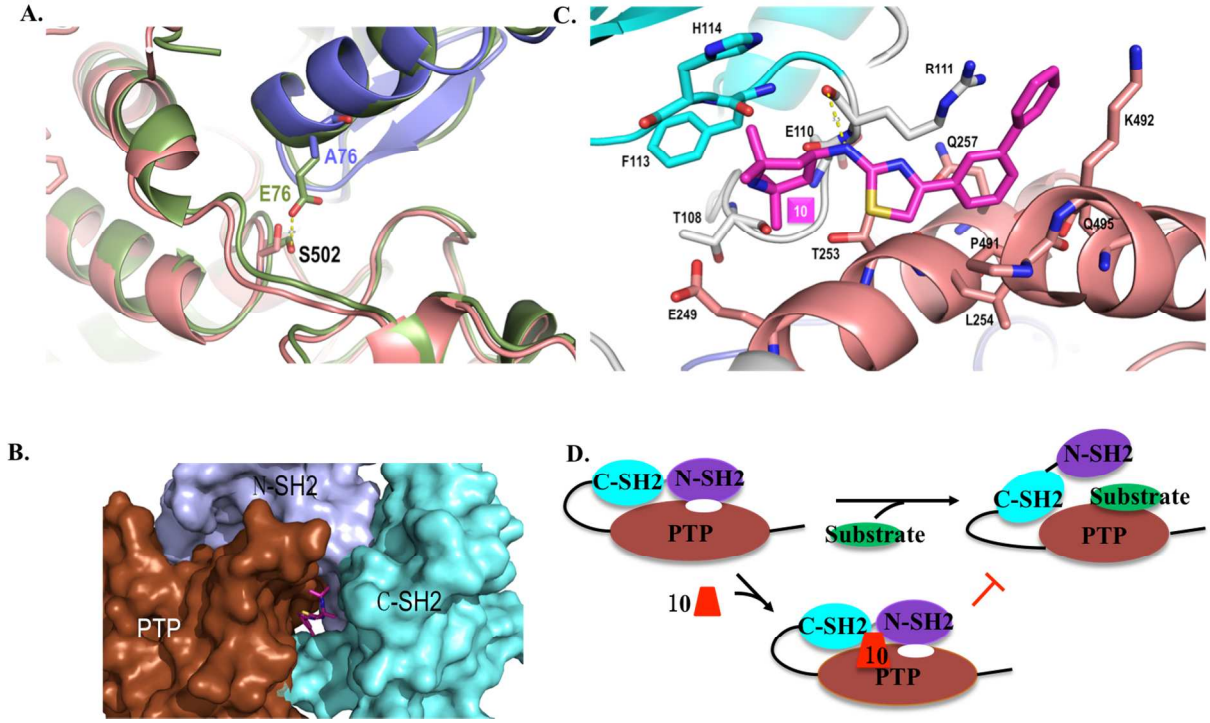


**Figure 3.** The structure of SHP2$^{E76A}$ in complex with **10** and a working model of allosteric inhibition of SHP2 $^{E76A}$ by **10**. **A**. The interaction between E76 and S502 in the structure of SHP2$^{WT}$(PDB code: 2SHP) in palegreen, which is absent in the structure of SHP2$^{E76A}$(purple) . **B. 10** settles in the central pocket formed by three domains as shown in surface representation. **C.** The complex structure of SHP2$^{E76A}$ and **10** (N-SH2 in lighblue; PTP in brown; C-SH2 in cyan). The allosteric inhibitor **10** is in magenta. **D**. A proposed model of conformational changes of SHP2$^{E76A}$ upon substrate binding and allosteric inhibition.

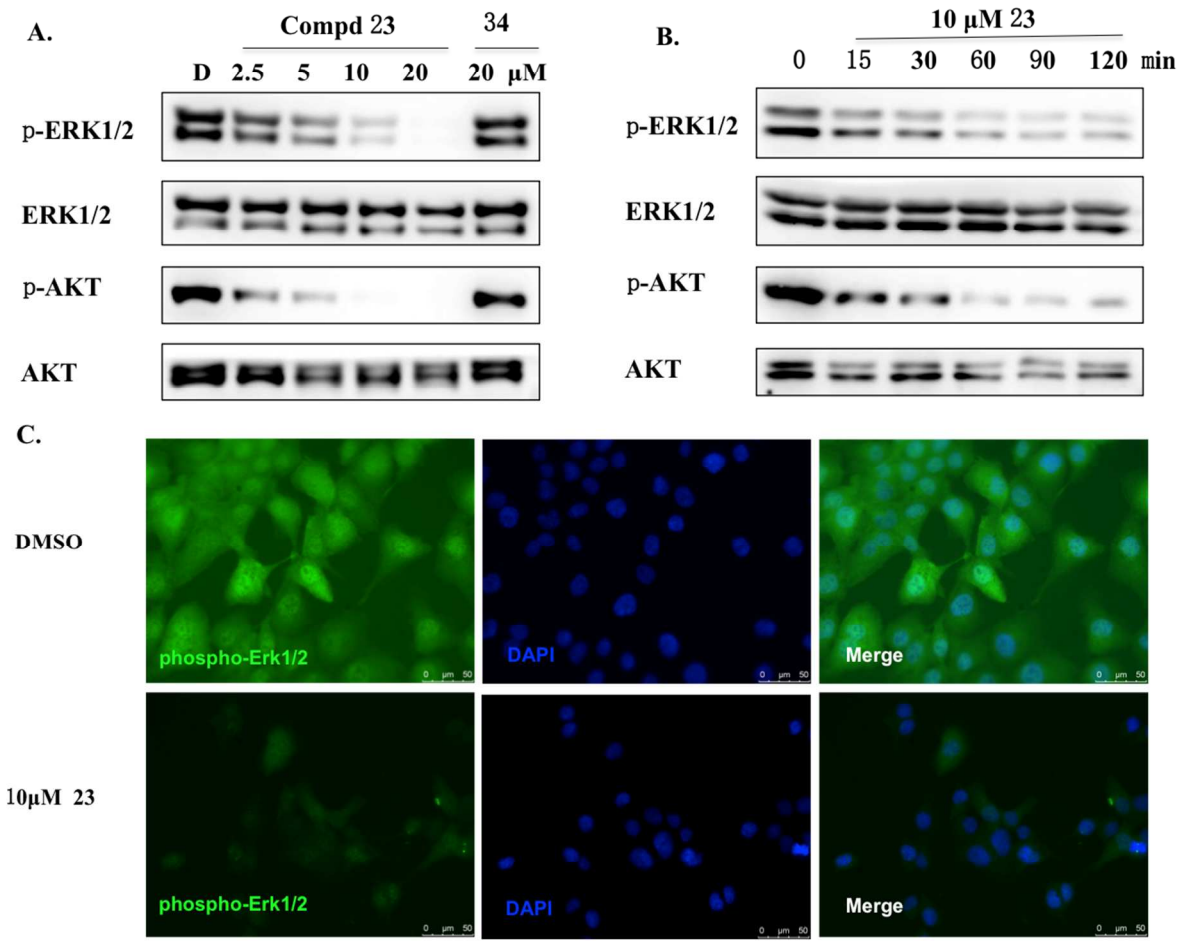


**Figure 4. 23** suppresses RAS-MAPK signaling pathway. **A.** Western blot of p-ERK1/2, ERK1/2, p-AKT and AKT from NCI-H661 cells treated with DMSO or indicated concentrations of **23** for 2 hours. **34** served as a negative control; **B.** Western blot of p-ERK1/2, ERK1/2, p-AKT and AKT from NCI-H661 cells treated with DMSO or 10μM **23** at different time points; **C.** NCI-H1975 cells treated with DMSO or 10μM **23** were stained with p-ERK1/2 antibody and DAPI. The scale bars represent 50μm.

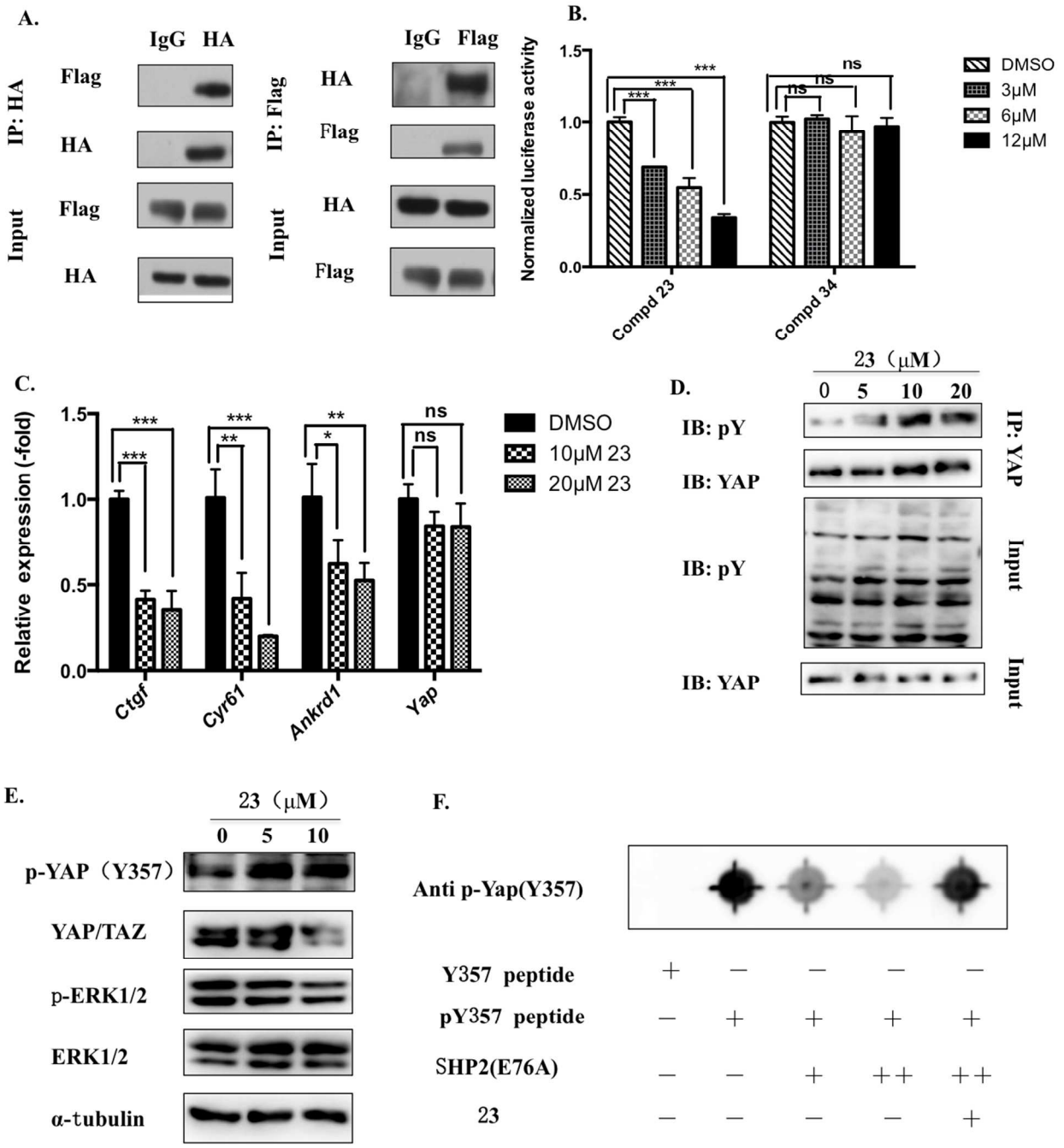


**Figure 5. 23** antagonizes YAP transcriptional activity and promotes phosphorylated Y357 of YAP. **A.** Interaction of SHP2 and YAP. Flag-YAP and HA-SHP2 were co-transfected into HEK293T cells. YAP and SHP2 interaction was examined by reciprocal co-immunoprecipitation as indicated; **B.** SF268 cells stably expressing a YAP-dependent luciferase reporter were treated with indicated concentrations of **23**. **34** served as a negative control. Normalized Luciferase=

Renilla luciferase/CellTiter-Glo. Error bars show mean±s.d. (n=3) *p<0.05, **p<0.01, ***p<0.001, ns: not significant; **C.** The qPCR analysis of *CTGF*, *CYR61*, *ANKRD1* and *YAP* mRNA levels in SF268 cells treated with DMSO and **23** for 2 hrs. Error bars show mean±s.d.(n=3) *p<0.05, **p<0.01, ***p<0.001, ns: not significant; **D.** SF268 cells were treated with DMSO or **23** at indicated concentrations for 2 hrs. The immunoprecipitates with anti-YAP antibody were analyzed by immunoblotting using pY-100 phosphotyrosine antibody. YAP harbors only one tyrosine residue in motif YXXP (tyrosine 357), which can be examined by pY-100 phosphotyrosine antibody; **E**. Western blot of indicated proteins from A549 cells treated with DMSO or **23** for 2 hours; **F.** *In vitro* dephosphorylation experiments were performed to examine the putative substrate of SHP2 using 357Y peptide (SGLSMSSYSVPRTPD), phosphorylated 357Y peptide (SGLSMSSpYSVPRTPD) of YAP and purified $SHP2^{E76A}$ protein. Dot blot results of indicated treatments were analyzed by p-YAP(Y357) antibody. 100μM pY357 peptide were incubated with 0.5nM $SHP2^{E76A}$ (+), 1.5nM $SHP2^{E76A}$ (++) for 15min and 20μM **23** was pretreated with 1.5nM $SHP2^{E76A}$ (++) for 15min before the peptide was added.

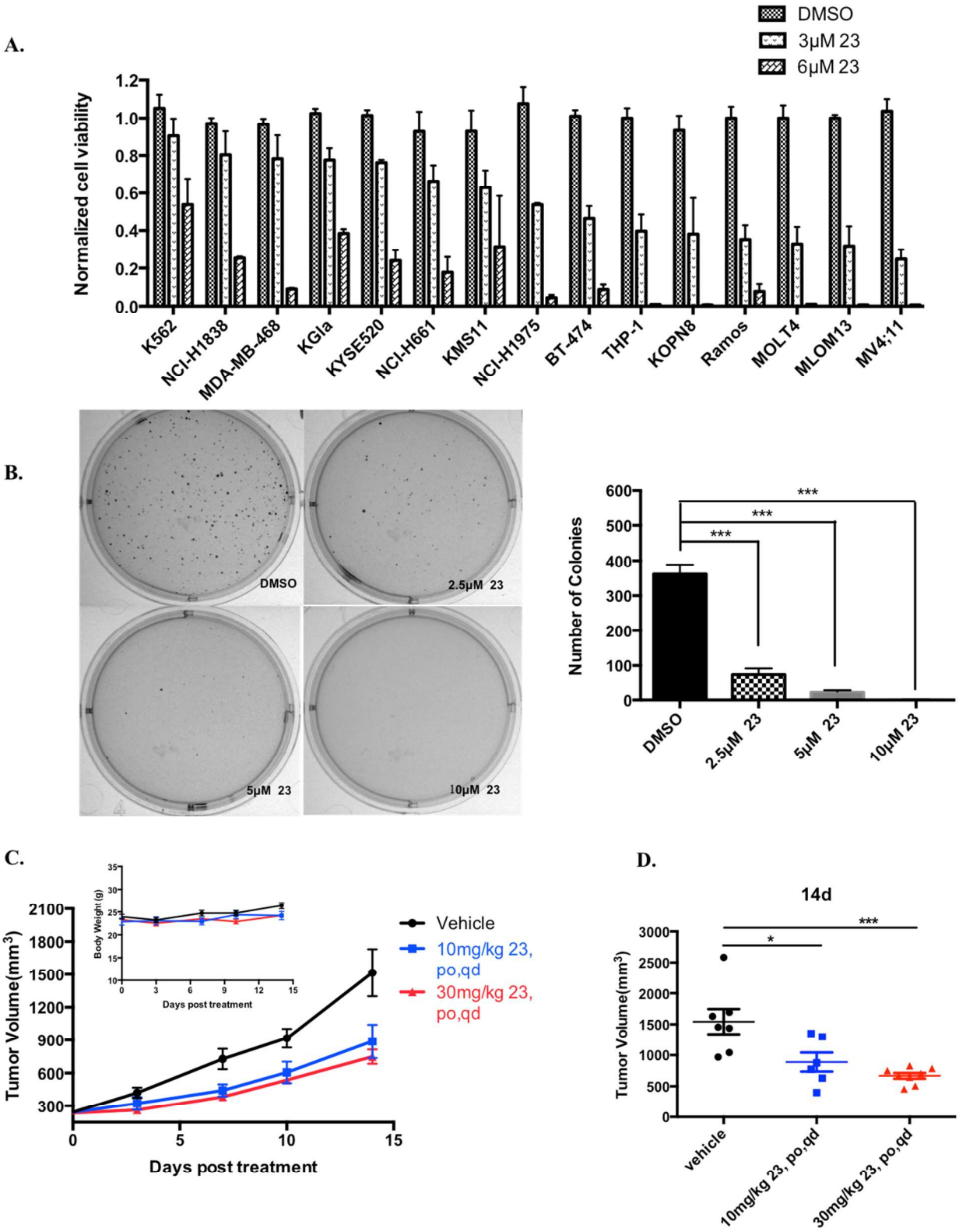
A.
DMSO
3μM 23
6μM 23
Normalized cell viability
1.2
1.0
0.8
0.6
0.4
0.2
0.0
K562
NCI-H1838
MDA-MB-468
KGIa
KYSE520
NCI-H661
KMS11
NCI-H1975
BT-474
THP-1
KOPN8
Ramos
MOLT4
MLOM13
MV4;11
B.
DMSO
2.5μM 23
5μM 23
10μM 23
Number of Colonies
600
500
400
300
200
100
0
***
***
***
DMSO
2.5μM 23
5μM 23
10μM 23
C.
Tumor Volume(mm3)
2100
1800
1500
1200
900
600
300
0
5
10
15
Days post treatment
Body Weight (g)
Days post treatment
Vehicle
10mg/kg 23, po,qd
30mg/kg 23, po,qd
D.
14d
Tumor Volume(mm3)
3000
2500
2000
1500
1000
500
0
*
***
vehicle
10mg/kg 23, po,qd
30mg/kg 23, po,qd

**Figure 6. 23** inhibits cancer cell proliferation *in vitro* and tumor growth *in vivo*. **A.** A panel of cancer cell lines was treated with **23** for 48hrs. Cell survival was measured by CellTiter-Glo. Data represent mean±s.d.(n=3); **B.** NCI-H1975 cells treated with **23** at indicated concentrations were subjected to a soft agar assay. The number of colonies is shown in graph. Error bars show mean±s.d.(n=3),***p<0.001; **C.** Efficacy study of **23** on MV4;11 xenograft tumor. Tumor volume was assessed by a caliper in two dimensions for mice treated with vehicle and **23** (10 mg/kg or 30 mg/kg, po, qd) twice weekly. Data represents mean±sem; (inset) Body weights of mice bearing MV4;11 xenografts. Body weight was measured twice a week for mice treated with vehicle and **23** (10mg/kg, 30mg/kg po, qd). Data represents mean±sem. **D.** Statistical significance of the antitumor effect on day 14. Data represents mean±sem **(***p<0.05, **p<0.01, ***p<0.001).

## SCHEMES

**Scheme 1. Synthesis of Compounds 9-19, 23 and 24.**[49]

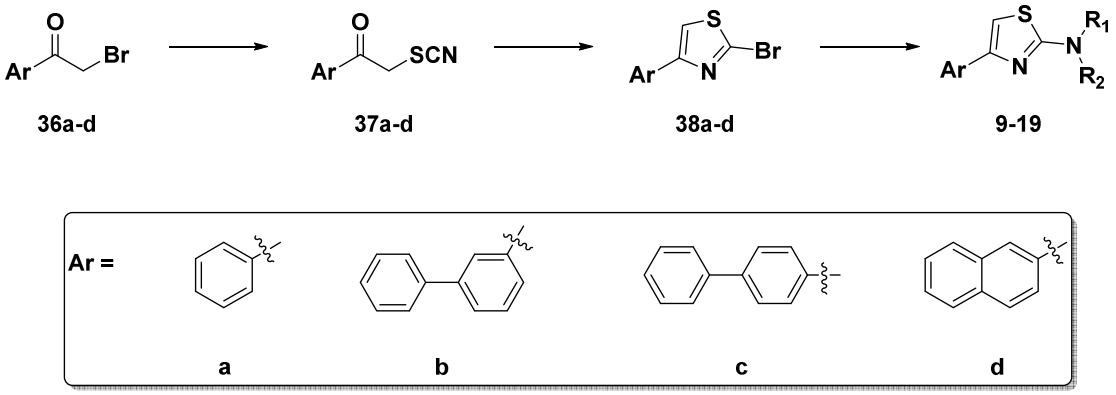

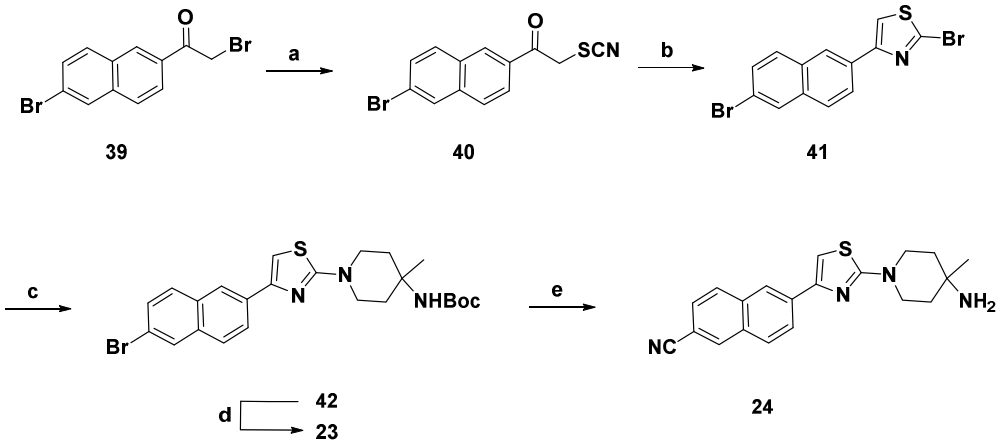


Reagents and conditions: (a) KSCN, EtOH, 85 $^{o}$C, 2h, 82-99%; (b) 30% HBr, AcOH, r.t., overnight, 78-90%; (c) $NHR_1R_2$, t-BuONa, Xantphos, $Pd_2(dba)_3$, toluene, 120 $^{o}$C, 2.5-16h, 32-52%; (d) TFA, DCM, r.t., 2h, 91%; (e) $Zn(CN)_2$, $Pd(PPh_3)_4$, DMF, 130 $^{o}$C, 8h, 31%.

**Scheme 2. Synthesis of Compounds 20-22, 25-35.**

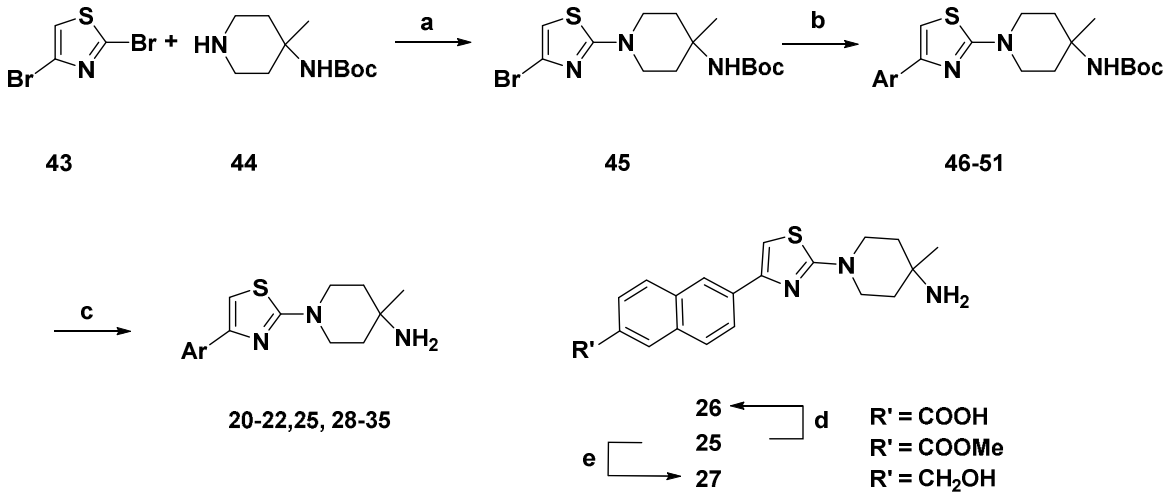

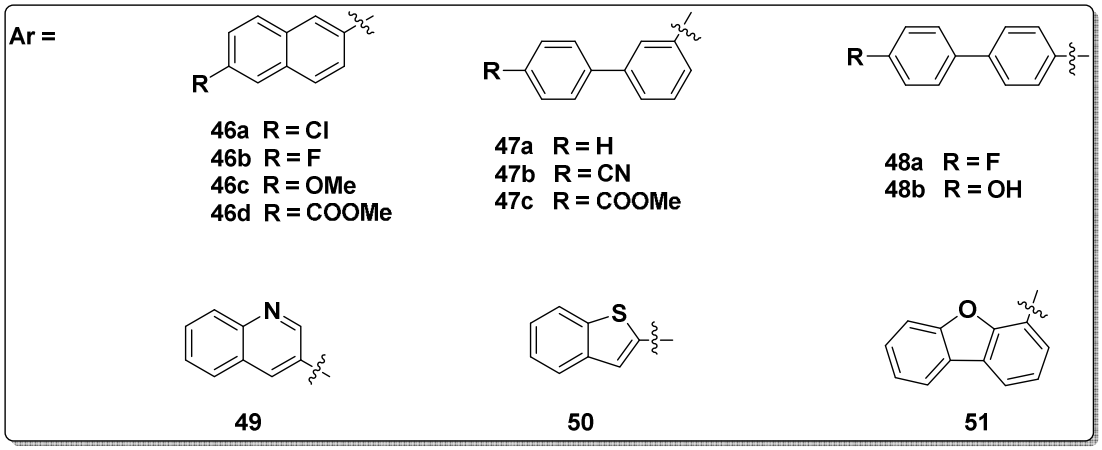


Reagents and conditions: (a) TEA, DMF, 90 °C, 8h, 87%; (b) $Na_2CO_3$, $Pd(PPh_3)_4$, THF:$H_2O$, 80 °C, 16h, 53-78%; (c) TFA, DCM, r.t. 1-5h, 85-96%; (d) KOH, 1,4-dioxane:$H_2O$, 70 °C, 1h, 86%; (e) $LiAlH_4$, THF, r.t., 3h, 76%.

## TABLES

**Table 1. Data Collection and Refinement Statistics**

| | SHP2 E76A |
|---|---|
| **Crystal parameters** | |
| Space group | $P2_12_12$ |
| Cell dimensions | |
| *a, b, c* (Å) | 55.8, 219.2, 41.3 |
| *α, β, γ* (˚) | 90, 90, 90 |
| Molecules in A.U.[a] | 1 |
| **Data collection** | |
| Synchrotron beamline | BL19U1 |
| Wavelength (Å) | 0.97853 |
| Resolution (Å) | 2.80 |
| Reflections | |
| Observed/ unique | 82892/24013 |
| Completeness (%) | 99.5 (99.7)[b] |
| $R_{merge}$ (%)[c] | 17.0 (58.2) |
| <I/σ> | 5.27 (1.63) |
| **Refinement** | |
| Resolution (Å) | 19.8 - 2.8 |

| | |
|---|---|
| $R_{work}$ (%)[d] | 24.0 |
| $R_{free}$ (%)[e] | 28.1 |
| No. of non-H atoms | |
| Protein | 4094 |
| Ligand | 28 |
| Water | 2 |
| R.m.s.deviation | |
| Bond length (Å) | 0.002 |
| Bond angle (˚) | 0.659 |
| **PDB accession code** | 5XZR |

a. A.U. = Asymmetric Unit
b. Values in parentheses correspond to the highest resolution shell.
*c.* $R_{merge} = \sum | I - \langle I \rangle | / \sum I$.
*d.* $R_{work} = \sum | F_O - F_C | / \sum F_O$.
*e.* $R_{free} = \sum | F_O - F_C | / \sum F_O$, calculated using a random set containing 5% reflections that were not included throughout structure refinement.

**Table 2. SAR of the amine region**

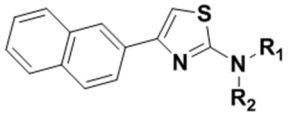

| ID | $NR_1R_2$ | $IC_{50}$ (μM) |
|---|---|---|
| **12** | 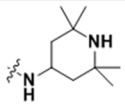 | 2.55±0.34 |
| **13** | 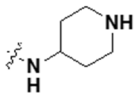 | 0.73±0.05 |
| **14** | 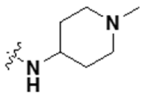 | 2.81±0.21 |
| **15** | 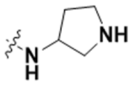 | 1.65±0.24 |
| **16** | 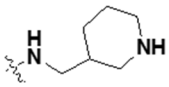 | 1.49±0.25 |
| **17** | 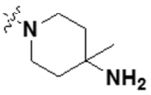 | 1.48±0.33 |
| **18** |  | 12.32±2.83 |
| **19** | 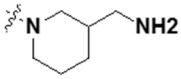 | 52.83±7.85 |

Each IC50 is at least the mean of 3 determinations

**Table 3. SAR of the aryl region**

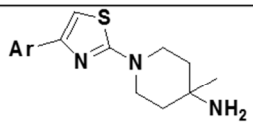


| ID | Ar | $IC_{50}$ (μM) | | ID | Ar | $IC_{50}$ (μM) |
|---|---|---|---|---|---|---|
| **20** | 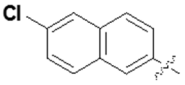 | 2.68±0.68 | | **28** | 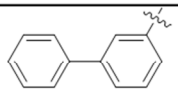 | 3.62±0.69 |
| **21** | 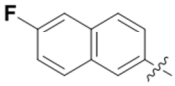 | 1.27±0.03 | | **29** | 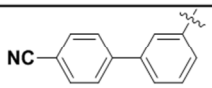 | 1.76±0.07 |
| **22** | 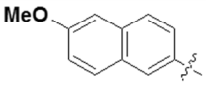 | 2.46±0.15 | | **30** | 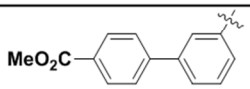 | 3.28±0.35 |
| **23** | 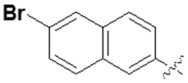 | 0.71±0.09 | | **31** | 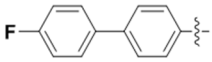 | 14.2±1.08 |
| **24** | 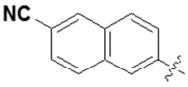 | 1.37±0.02 | | **32** | 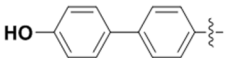 | 20.3±2.02 |
| **25** | 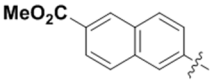 | 1.08±0.07 | | **33** | 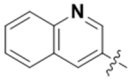 | 52.3±5.82 |
| **26** | 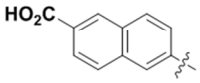 | 51.7±6.71 | | **34** | 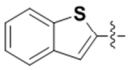 | >100 |
| **27** | 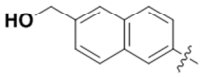 | >100 | | **35** | 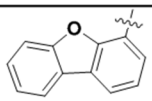 | 46.5±3.47 |

Each IC50 is at least the mean of 3 determinations

**Table 4. Selectivity of 23 against a panel of phosphatases**

| Phosphatase | IC50(μM) |
|---|---|
| LmwPTP | >100 |
| MKP3 | >100 |
| PTP1B | 31.23±1.82 |
| TC-PTP | >100 |
| SHP1 | 34.62±3.91 |
| VHR | >100 |
| CDC25A | 27.46±2.01 |
| $SHP2^{E76A}$ | 0.71±0.09 |

Each IC50 is at least the mean of 3 determinations

# Table of Contents graphic